

# Some Notes on the Physics of Type Ia Supernovae using Elementary Methods

E. D. Commins     September, 2002

## 1. Introduction

The typical Type Ia supernova explosion is an extremely complex phenomenon. The progenitor star is thought to be a carbon/oxygen white dwarf driven close to the Chandrasekhar limit by accretion from a binary companion, (although this is not certain). At sufficiently high central density and temperature a thermonuclear instability is initiated at or near the center of the progenitor. It is thought that at first it spreads relatively slowly (deflagration), but ultimately propagates supersonically (detonation). The thermonuclear reaction network is very complex; starting with carbon and oxygen, it extends through intermediate mass nuclides such as neon, magnesium, silicon, sulfur, calcium, and titanium, and ultimately terminates in the generation of large quantities of  $^{56}\text{Ni}$ . Neutrino losses are very important throughout the explosion, as are hydrodynamical instabilities over a very wide range of length scales.

The explosion ejecta fly off with extremely high speeds ( $\approx 10^4$  km/sec), the total energy release being  $\approx 10^{51}$  ergs. The optical luminosity in the weeks after the explosion is powered by the radioactive decay of  $^{56}\text{Ni}$  to  $^{56}\text{Co}$ , and then  $^{56}\text{Co}$  to  $^{56}\text{Fe}$ . The degradation of gamma-ray and positron energy from these radioactive decays to generate optical luminosity involves an intricate network of processes, including Compton scattering, photo-ionization, ionization and excitation by Compton primary and secondary electron impact, heating by electron-electron scattering, and various forms of recombination. The opacity of the hot, partially ionized, expanding plasma involves not only electron scattering, free-free and bound-free transitions, but also hundreds of thousands of “bound-bound” atomic transitions, where the Doppler effect arising from the high velocities of expansion plays an essential role in broadening the atomic lines.

Given this overwhelming complexity, it is quite miraculous that Type Ia supernovae form such a homogeneous set of objects, with so much regularity in their light curves and spectra. Is it possible that, in spite of the underlying complexity, the essence of these regularities can be explained by relatively simple spherically symmetric models involving “elementary” physics and a minimum of “black-box” computer code? We do not know if this is the case, but the possibilities are certainly worth exploring. In these notes we will try to see what we can understand about Type Ia supernovae from a naïve and simple-minded approach.

## 2. Properties of White dwarf configurations

### 2.1 Elementary “derivation” of the Chandrasekhar limit.

Let us start by assuming that the progenitor star is a carbon/oxygen white dwarf. These are very common objects: the left-over cores of red giant stars (with original masses in the range  $2-8 M_{\odot}$ ) that have shed their envelopes by well-known processes of mass loss. Since  $\approx 40\%$  of all known stars appear in binary systems, we may assume that many C/O white dwarfs are also members of binary pairs.

The typical C/O white dwarf has a mass of .6-.7  $M_{\odot}$ , but a radius comparable to that of the earth. Thus the mass density is enormous ( $\approx 10^{4-6}$  g/cm<sup>3</sup> or more) and is supported against gravitational crush by electron degeneracy pressure, rather than by ordinary gas pressure or radiation pressure. Let's now explain how this works in the simplest possible way. According to Fermi-Dirac statistics, the number of electrons per unit volume for an ideal degenerate electron gas at temperature T is:

$$n_e = \frac{1}{\pi^2 \hbar^3} \int_0^{\infty} \frac{p^2 dp}{\exp\left(\frac{E - \mu}{kT}\right) + 1} \quad (2.1)$$

where p is the electron momentum, E is the energy, and  $\mu$  is the chemical potential. Now in a quiescent white dwarf star the internal temperature might be  $\approx 10^8$  K; on the other hand the electron density is so high that  $\mu/k$  is orders of magnitude larger. In this case it is appropriate to make the "zero temperature approximation" in which  $\mu \rightarrow \mu_F = \mu(T=0)$ , and:

$$\begin{aligned} \frac{1}{\exp\left(\frac{E - \mu}{kT}\right) + 1} &\rightarrow 1 \quad \text{if } E < \mu_F \\ &\rightarrow 0 \quad \text{if } E > \mu_F \end{aligned}$$

Hence, in the zero temperature limit (2.1) becomes:

$$n_e = \frac{1}{\pi^2 \hbar^3} \int_0^{p_F} p^2 dp = \frac{p_F^3}{3\pi^2 \hbar^3} \quad (2.2)$$

where  $p_F$  is the "Fermi momentum" corresponding to the Fermi energy  $\mu_F$ . Inverting (2.2) we obtain:

$$p_F = (3\pi^2 \hbar^3 n_e)^{1/3} \approx \hbar \cdot n_e^{1/3} \quad (2.3)$$

The kinetic energy per unit volume in the zero temperature approximation is:

$$\varepsilon = \frac{1}{\pi^2 \hbar^3} \int_0^{p_F} E p^2 dp \quad (2.4)$$

If the electrons are non-relativistic,  $E=p^2/2m_e$  and (2.4) becomes:

$$\varepsilon = \frac{1}{2\pi^2 \hbar^3 m_e} \int_0^{p_F} p^4 dp = \frac{p_F^5}{10\pi^2 \hbar^3 m_e} \quad (2.5)$$

Substituting (2.3) in (2.5) we obtain:

$$\varepsilon \approx \frac{\hbar^2}{m_e} n_e^{5/3} \quad (2.6)$$

The pressure  $P$  of a non-relativistic ideal gas is always  $2/3$  of the kinetic energy density. Hence from (2.6) we find:

$$P \approx \frac{\hbar^2}{m_e} n_e^{5/3} \quad (2.7)$$

Now the electron number density is related to the mass density  $\rho$  as follows. For each nucleus with atomic number  $Z$  and mass number  $A$ , there must be  $Z$  electrons (all pressure ionized and thus “free”) by charge neutrality. Hence, for a single nuclear species we can write:  $n_e = Zn_N = \frac{Z\rho}{Am_p}$ . More generally, if there are several nuclear species, we

have:  $n_e = \frac{\rho}{\mu_e m_p}$  where  $\mu_e^{-1}$  is the ratio of protons to nucleons in the whole gas. For a C/O white dwarf,  $\mu_e^{-1}=1/2$ . Thus, from (2.7) we can write:

$$P \approx \frac{\hbar^2}{m_e} \frac{\rho^{5/3}}{m_p^{5/3}} \quad (2.8)$$

Mechanical equilibrium between gravitation and pressure is expressed by the equation of hydrostatic equilibrium:

$$\frac{\partial P}{\partial r} = -\frac{GM(r)\rho}{r^2} \quad (2.9)$$

Here  $G$  is Newton’s constant, and  $M(r)$  is the mass interior to a radius  $r$  measured from the center of the star. To get an intuitive feeling for (2.9), we replace the derivative by:

$$\frac{P(R) - P(0)}{R} = \frac{-P(0)}{R}$$

and  $M(r)$  by  $M(R)=M$ . Here  $R$  is the star radius, and  $M$  is the total mass. Also we write:

$$\rho \approx \frac{M}{R^3} \quad (2.10)$$

Then, (2.9) becomes:

$$P(0) \approx \frac{GM^2}{R^4} \quad (2.11)$$

Employing (2.8) for the pressure, we get the relation:

$$\frac{\hbar^2}{m_e m_p^{5/3}} \frac{M^{5/3}}{R^5} \approx \frac{GM^2}{R^4} \quad (2.12)$$

We can re-arrange this equation to express R in terms of the mass M. Inserting numerical values for the various constants, we find:

$$R \approx 6 \cdot 10^8 \left( \frac{M_{sun}}{M} \right)^{1/3} \text{ cm} \quad (2.13)$$

This tells us that for a non-relativistic white dwarf, the radius varies as the (-1/3) power of the mass. We can also find how the density varies with M, by substituting (2.10) in (2.13). This yields:

$$\rho \approx 1 \cdot 10^7 \left( \frac{M}{M_{sun}} \right)^2 \text{ gm/cm}^3 \quad (2.14)$$

Thus, as we add mass in the non-relativistic approximation, the density increases. But then the Fermi momentum must also increase and eventually reach  $m_e c$ , in which case the non-relativistic approximation must break down. Recalling (2.3), we see that this occurs when:

$$m_e c \approx \hbar n_e^{1/3}$$

or:

$$n_e \approx \left( \frac{m_e c}{\hbar} \right)^3 \quad (2.15)$$

This simply means that relativistic effects begin to become important when the spacing between the electrons is of the order of the Compton wavelength ( $3.8 \cdot 10^{-11}$  cm). The corresponding mass density is:

$$\rho = \mu_e m_p n_e \approx m_p \left( \frac{m_e c}{\hbar} \right)^3 \approx 10^7 \text{ gm/cm}^3 \quad (2.16)$$

Comparing (2.16) and (2.14) we see that the non-relativistic approximation breaks down when  $M \approx 1 M_{\odot}$ .

If we continue to add mass, the electrons become more and more relativistic. Ultimately they will be ultra-relativistic: each with kinetic energy  $E=pc$ . In this case, from (2.4) the energy density of the electron gas will be:

$$\varepsilon = \frac{1}{\pi^2 \hbar^3} \int_0^{p_F} c p \cdot p^2 dp = \frac{c p_F^4}{4 \pi^2 \hbar^3} \quad (2.17)$$

Recalling that  $p_F \approx \hbar n_e^{1/3}$  and that for an ultra-relativistic ideal gas, the pressure is always 1/3 of the kinetic energy density, we see that :

$$P \approx \hbar c \left( \frac{\rho}{m_p} \right)^{4/3} \approx \frac{\hbar c}{m_p^{4/3}} \frac{M^{4/3}}{R^4} \quad (2.18)$$

From the equation of hydrostatic equilibrium in the form of (2.11), we have:

$$\frac{\hbar c}{m_p^{4/3}} \frac{M^{4/3}}{R^4} = \frac{GM^2}{R^4} \quad (2.19)$$

This time R appears to the minus 4'th power on both sides of the equation; hence we have a solution for only one value of M:

$$M_C \approx \left( \frac{\hbar c}{G} \right)^{3/2} \frac{1}{m_p^2} \quad (2.20)$$

Thus we arrive at an approximate formula for the Chandrasekhar limit, which occurs when all the electrons are ultra-relativistic. A proper derivation, given in the next section, yields the same quantity on the right hand side of (2.20), multiplied by a numerical factor which is very nearly unity.

## 2.2 More detailed treatment of the Chandrasekhar Limit.

Let's now try to be somewhat more precise. Our starting point is the basic kinetic theory formula for the pressure in a gas, expressed in terms of the velocity v and momentum p of a typical particle in the gas:

$$\begin{aligned} P &= \frac{1}{3} \langle vp \rangle = \frac{1}{3} \left\langle p \frac{\partial E}{\partial p} \right\rangle \\ &= \frac{1}{3} \left\langle \frac{c^2 p^2}{E} \right\rangle \end{aligned} \quad (2.21)$$

where now  $E = mc^2 \sqrt{1 + \frac{p^2}{m^2 c^2}}$ . For a zero-temperature Fermi-Dirac ideal gas, (2.21) becomes:

$$\begin{aligned} P &= \frac{c^2}{3\pi^2 \hbar^3} \int_0^{p_F} \frac{p^4 dp}{E} \\ &= \frac{m^4 c^5}{3\pi^2 \hbar^3} \int_0^x \frac{z^4 dz}{\sqrt{1+z^2}} \end{aligned} \quad (2.22)$$

where  $x = p_F / mc$ . By making the substitution  $z = \sinh \theta$  in the integrand, we easily evaluate the integral in the second line of (2.22) and arrive at the formula

$$P = A \left[ x(2x^2 - 3)(x^2 + 1)^{1/2} + 3 \sinh^{-1} x \right] \quad (2.23)$$

where

$$A = \frac{8\pi^4 m^4 c^5}{3\hbar^3} = 6.01 \cdot 10^{22} \quad (\text{in cgs units}) \quad (2.24)$$

In Fig. 1 we plot the pressure as a function of  $x$ . Note that for  $x \ll 1$ ,  $P \rightarrow 8Ax^5/5$ , while for  $x \gg 1$ ,  $P \rightarrow 2Ax^4$ .

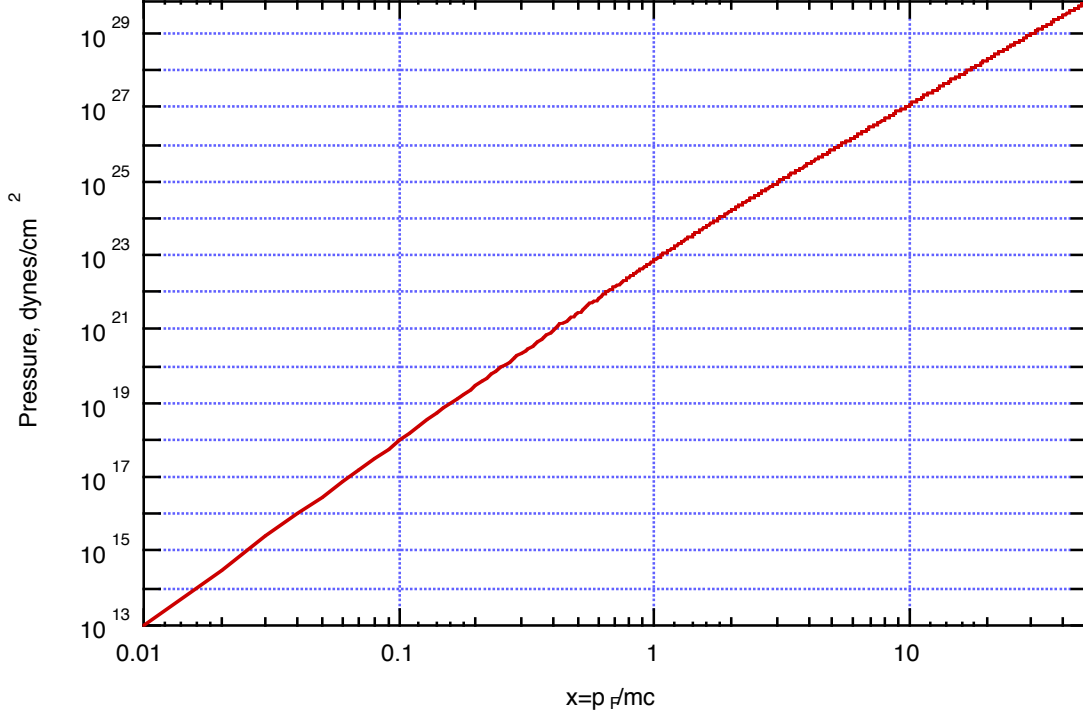


Fig.1 The pressure in a zero temperature ideal Fermi gas, versus the Fermi momentum in units of  $mc$ .

Now, from (2.22) and the equation of hydrostatic equilibrium, we have:

$$\frac{\partial P}{\partial r} = \frac{\partial P}{\partial x} \frac{\partial x}{\partial r} = \frac{m^4 c^5}{3\pi^2 \hbar^3} \frac{x^4}{\sqrt{1+x^2}} \frac{\partial x}{\partial r} = -\frac{GM(r)\rho}{r^2} \quad (2.25)$$

Meanwhile, from (2.2),

$$n_e = \frac{p_F^3}{3\pi^2 \hbar^3} = \frac{m^3 c^3}{3\pi^2 \hbar^3} x^3 \quad (2.26)$$

and

$$\rho = \mu_e m_p n_e = \mu_e m_p \frac{m^3 c^3}{3\pi^2 \hbar^3} x^3 = Bx^3 \quad (2.27)$$

where  $B = 9.82 \cdot 10^5 \mu_e$  in cgs. Therefore, (2.25) becomes:

$$\frac{mc^2}{\mu_e m_p G} \frac{x}{\sqrt{1+x^2}} \frac{\partial x}{\partial r} = -\frac{M(r)}{r^2} \quad (2.28)$$

which can be written as:

$$\frac{mc^2}{\mu_e m_p G} \frac{\partial}{\partial r} \sqrt{1+x^2} = -\frac{M(r)}{r^2} \quad (2.29)$$

It's convenient at this point to make the substitution  $y=(1+x^2)^{1/2}$  so that (2.29) becomes:

$$\frac{mc^2}{\mu_e m_p G} r^2 \frac{\partial y}{\partial r} = -M(r) \quad (2.30)$$

Differentiating both sides of (2.30), recalling that

$$\frac{\partial M(r)}{\partial r} = 4\pi r^2 \rho$$

and using (2.27) again, we obtain:

$$\frac{1}{r^2} \frac{\partial}{\partial r} \left( r^2 \frac{\partial y}{\partial r} \right) = -\frac{4(\mu_e m_p)^2 G m^2 c}{3\pi \hbar^3} (y^2 - 1)^{3/2} \quad (2.31)$$

We now make the further substitutions  $y=y_0\phi$  where  $\phi(0)=1$ , and  $r=a\eta$  where:

$$\begin{aligned} a &= \left[ \frac{3\pi \hbar^3}{4\mu_e^2 m_p^2 G m^2 c} \right]^{1/2} \frac{1}{y_0} \\ &= \frac{7.71 \cdot 10^8}{\mu_e y_0} \text{ cm} \end{aligned}$$

Then (2.31) becomes:

$$\frac{1}{\eta^2} \frac{\partial}{\partial \eta} \left( \eta^2 \frac{\partial \phi}{\partial \eta} \right) = -\left( \phi^2 - \frac{1}{y_0^2} \right)^{3/2} \quad (2.32)$$

This is Chandrasekhar's equation, the solutions of which describe the run of the function  $\phi$  for various  $y_0$ . The quantity  $\phi$  varies from the value unity at the origin to  $1/y_0^2$  at the

outer radius  $\eta_1$ . The density is  $\rho = Bx^3 = B(y^2 - 1)^{3/2} = By_0^3 \left( \phi^2 - \frac{1}{y_0^2} \right)^{3/2}$  ; it vanishes at  $\eta_1$ .

The mass of the white dwarf is:

$$\begin{aligned}
 M &= 4\pi \int_0^R r^2 \rho dr \\
 &= 4\pi a^3 B y_0^3 \int_0^{\eta_1} \eta^2 \left( \phi^2 - \frac{1}{y_0^2} \right)^{3/2} d\eta \\
 &= 4\pi a^3 B y_0^3 \int_0^{\eta_1} -\frac{\partial}{\partial \eta} (\eta^2 \phi) d\eta \\
 &= 4\pi a^3 B y_0^3 \eta_1^2 \left( -\frac{\partial \phi}{\partial \eta} \right)_{\eta_1} \\
 &= \frac{.122}{\mu_e^2} \left( \frac{\hbar c}{G} \right)^{3/2} \frac{1}{m_p^2} \eta_1^2 \left( -\frac{\partial \phi}{\partial \eta} \right)_{\eta_1}
 \end{aligned} \tag{2.33}$$

Although  $y_0$  does not appear explicitly in this expression, it does enter implicitly, since the function  $\phi$  depends on  $y_0$ . Numerical integration of (2.32) for various values of  $y_0$  yields the following results:

- When  $y_0 \rightarrow \infty$ , the central density becomes infinite, but the total mass reaches the finite limiting value (Chandrasekhar limit):

$$\begin{aligned}
 M_C &= 5.75 \mu_e^{-2} M_\odot \\
 &= 1.438 M_\odot \text{ for } \mu_e = 2.
 \end{aligned} \tag{2.34}$$

Fig. 2 is a plot of the central density as a function of  $M/M_C$ .



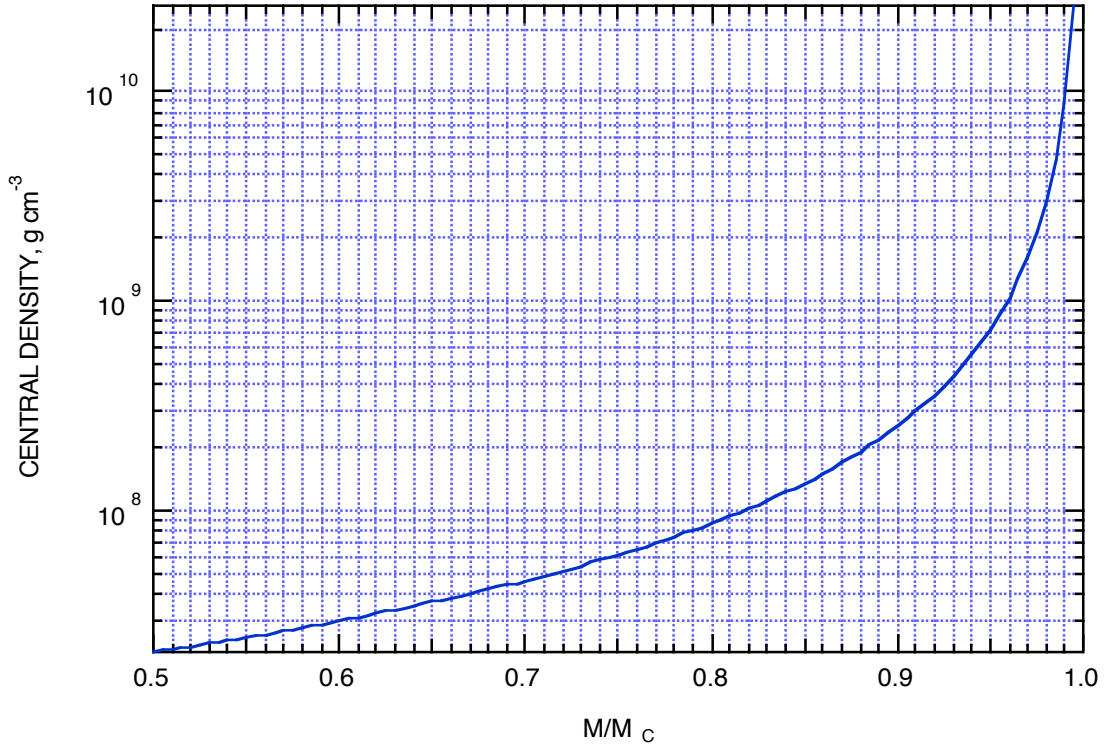


Fig.2. Central density of a zero temperature white dwarf as a function of  $M/M_C$ . ( $\mu_e=2$ ).

Here are several reasonably accurate numerical formulae, valid for  $\mu_e=2$ . The central density is:

$$\begin{aligned} \rho_0 &= 1.964 \cdot 10^6 (y_0^2 - 1)^{3/2} \\ &\approx 7.17 \cdot 10^6 \left( \frac{1}{1 - \frac{M}{M_C}} \right)^{1.546} \text{ g cm}^{-3} \end{aligned} \quad (2.35)$$

$M$  (in solar masses) as a function of  $y_0$ , is:

$$M = -3.1967 + \frac{4.636}{1 + \frac{.44973}{y_0^{1.4793}}} \quad (2.36)$$

This yields  $M_C=1.4393$  solar masses in the limit of large  $y_0$ . The inverse relation is:

$$y_0 = .5826 \left[ \frac{\frac{M}{M_C} + 2.221}{1 - \frac{M}{M_C}} \right]^{.676} \quad (2.37)$$

• As  $M$  approaches  $M_C$  the radius decreases. This is illustrated in Fig. 3, and also in Fig.4.

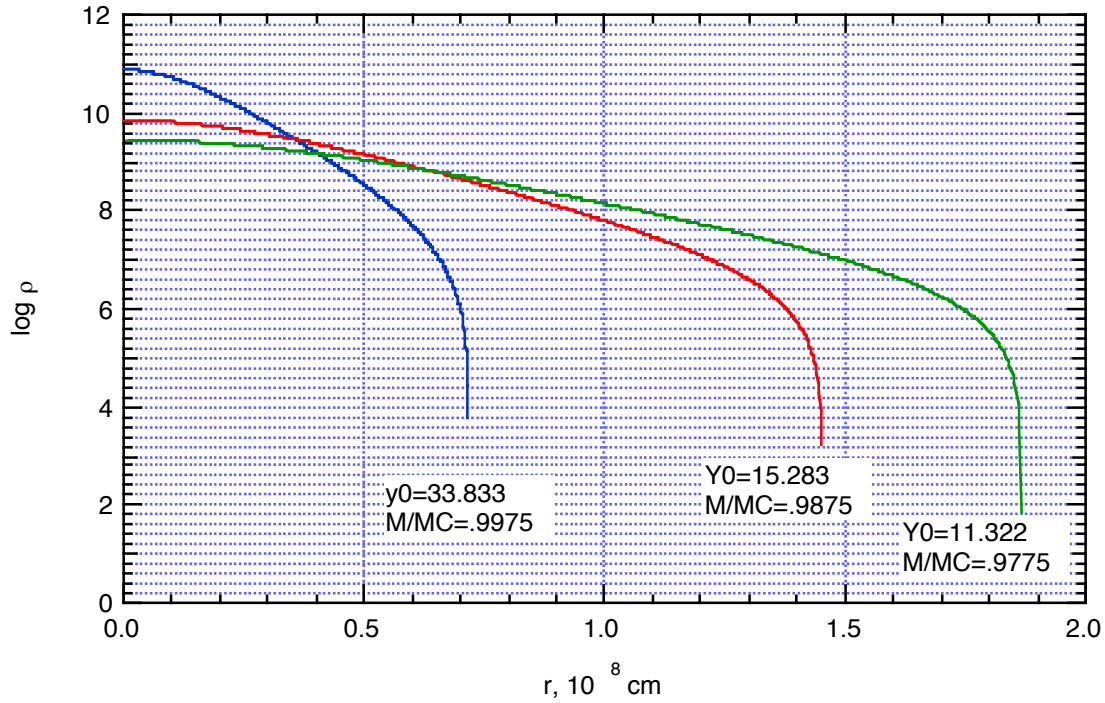


Fig. 3. Plot of density versus radial distance from center for various values of  $M/M_C$ .

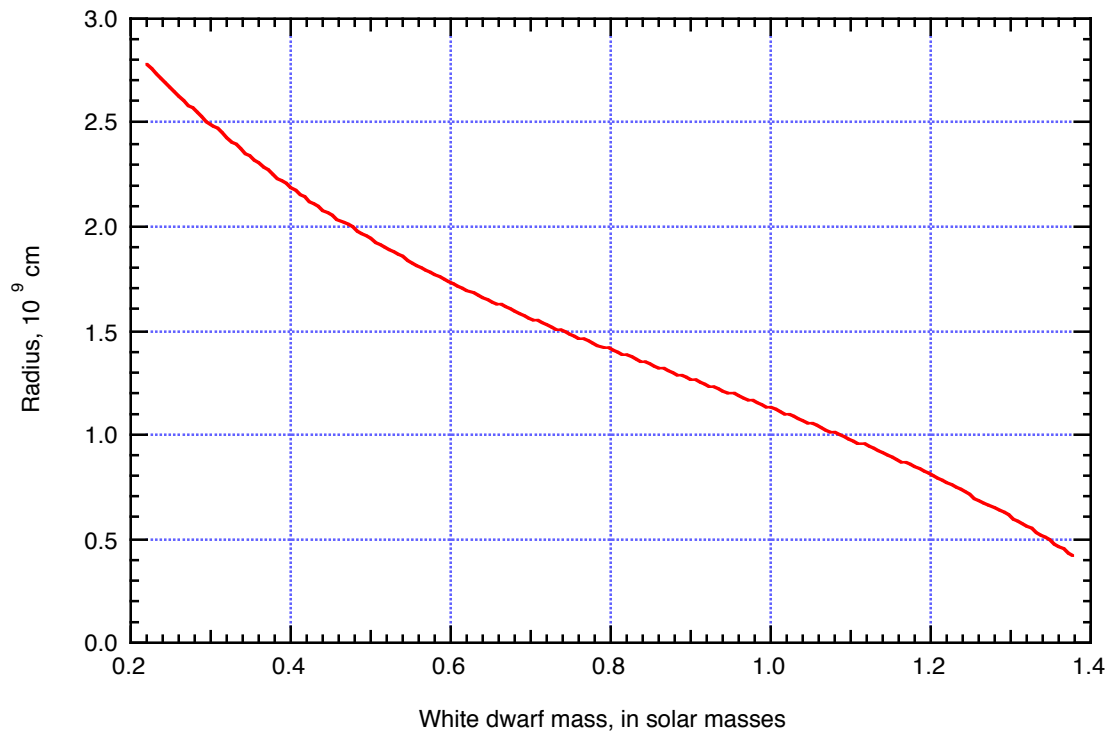


Fig.4 White dwarf radius versus mass

Of course the zero-temperature Chandrasekhar theory represents an idealized situation, and various corrections are necessary to make it more realistic. These include corrections for Coulomb, General Relativistic, and electron-capture effects. We won't go into any

detail about these, but merely state that they reduce very slightly the limiting mass (by  $\approx 1\%$ ) and make the central density at the limiting mass very large but finite.

### 2.3 The energy of a zero-temperature white dwarf.

The mass interior to radius  $r$  satisfies the equation:

$$\frac{\partial M(r)}{\partial r} = 4\pi r^2 \rho \quad (2.42)$$

Making use of this formula in equation (2.9) we have the equation of hydrostatic equilibrium in the following form:

$$\frac{\partial P}{\partial r} = -\frac{GM(r)}{4\pi r^4} \frac{\partial M(r)}{\partial r} \quad (2.43)$$

Let's multiply both sides of (2.43) by  $4\pi r^3$  and integrate from 0 to  $R$ :

$$\int_0^R 4\pi r^3 \frac{\partial P}{\partial r} dr = -G \int \frac{M(r) dM(r)}{r} \quad (2.44)$$

The right hand side of (2.44) is just the gravitational potential energy  $\Omega$  of the star. Integrating the left hand side by parts, we see that (2.44) is:

$$\int 3PdV = -\Omega \quad (2.45)$$

Now, if the white dwarf has  $M \ll M_C$ , it is non-relativistic throughout, in which case  $P=2\varepsilon/3$  where  $\varepsilon$  is as usual the kinetic energy density. Defining the thermal energy as  $U=\int \varepsilon dV$ , we thus have for a non-relativistic cold white dwarf:

$$2U + \Omega = 0 \quad (2.46)$$

The total energy of the star (disregarding electron and nuclear rest energy) is  $E=U+\Omega$ . We see from (2.46) that in the non-relativistic case,  $E=-U=\Omega/2$ . (Of course this is just the virial theorem). What happens if we let  $M \rightarrow M_C$ ? Here the electrons become ultra-relativistic, in which case  $P \rightarrow \varepsilon/3$ . Thus it would appear that in the ultra-relativistic limit,  $U+\Omega \rightarrow 0$ . However, we must be careful in taking this limit, since when  $M \rightarrow M_C$ ,  $U \rightarrow \infty$ , while at the same time  $\Omega \rightarrow -\infty$ . Now,  $U$  is obviously given by the following expression:

$$U = \int dV \frac{1}{\pi^2 \hbar^3} \int_0^{p_F} (\sqrt{p^2 c^2 + m^2 c^4} - mc^2) p^2 dp \quad (2.47)$$

Meanwhile, from (2.22) we have the formula:

$$3P = \frac{1}{\pi^2 \hbar^3} \int_0^{p_F} c^2 \frac{p^4}{\sqrt{p^2 c^2 + m^2 c^4}} dp \quad (2.48)$$

Hence, the total energy, excluding rest energy, is  $E=U-\int 3PdV$ :

$$\begin{aligned}
E &= \int dV \frac{m^4 c^5}{\pi^2 c^3} \int_0^x \left[ \frac{z^2}{\sqrt{1+z^2}} - z^2 \right] dz \\
&= 4\pi a^3 \cdot \frac{m^4 c^5}{\pi^2 \hbar^3} \cdot \int_0^{n_1} \eta^2 d\eta \left[ \frac{1}{2} \left( x\sqrt{1+x^2} - \ln(x + \sqrt{1+x^2}) \right) - \frac{x^3}{3} \right]
\end{aligned} \tag{2.49}$$

where as we have noted,  $a=3.855 \cdot 10^8 y_0^{-1}$  cm for  $\mu_e=2$ , and  $x = \frac{P_F}{mc} = [y_0^2 \phi^2 - 1]^{1/2}$ . We have evaluated the integral in (2.44) numerically for various  $y_0$ ; the results, expressed in terms of the energy  $E_{50}$  in  $10^{50}$  ergs are shown in Fig. 5.

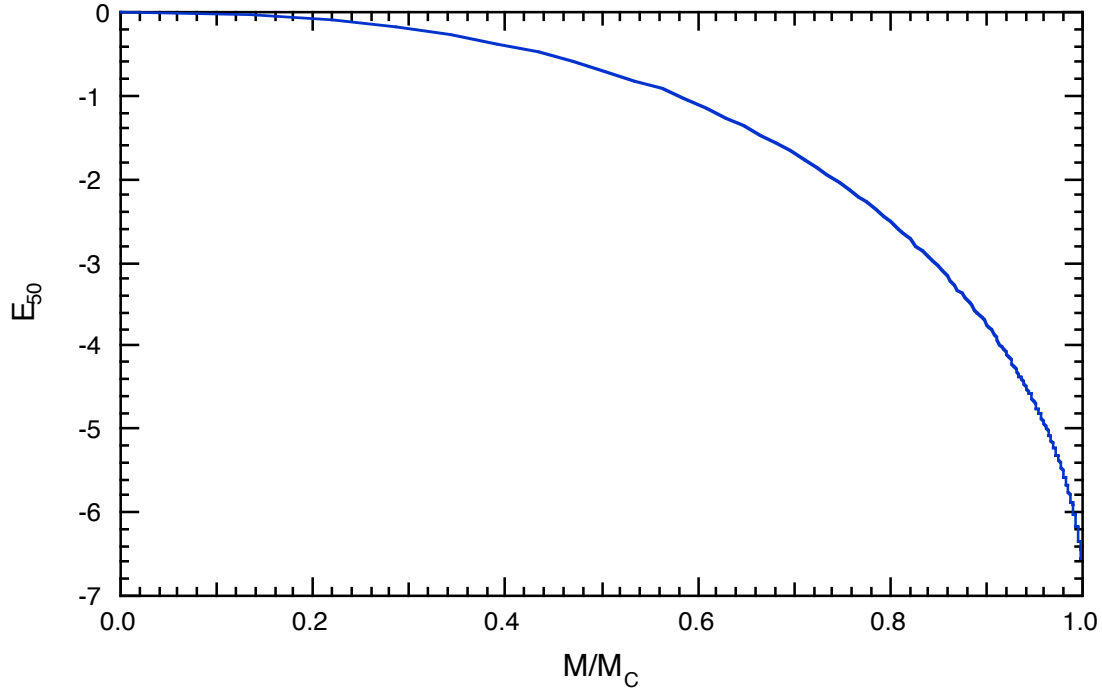


Fig. 5. The energy  $E$  in units of  $10^{50}$  ergs, plotted versus  $M/M_C$ .

#### 2.4 How good is the zero-temperature approximation?

The zero temperature approximation should be valid so long as

$$\mu_F \equiv kT_F \gg kT \tag{2.50}$$

We have calculated  $T_F$  versus  $r$  for a number of cold white dwarf configurations. The results are shown in Fig. 6.

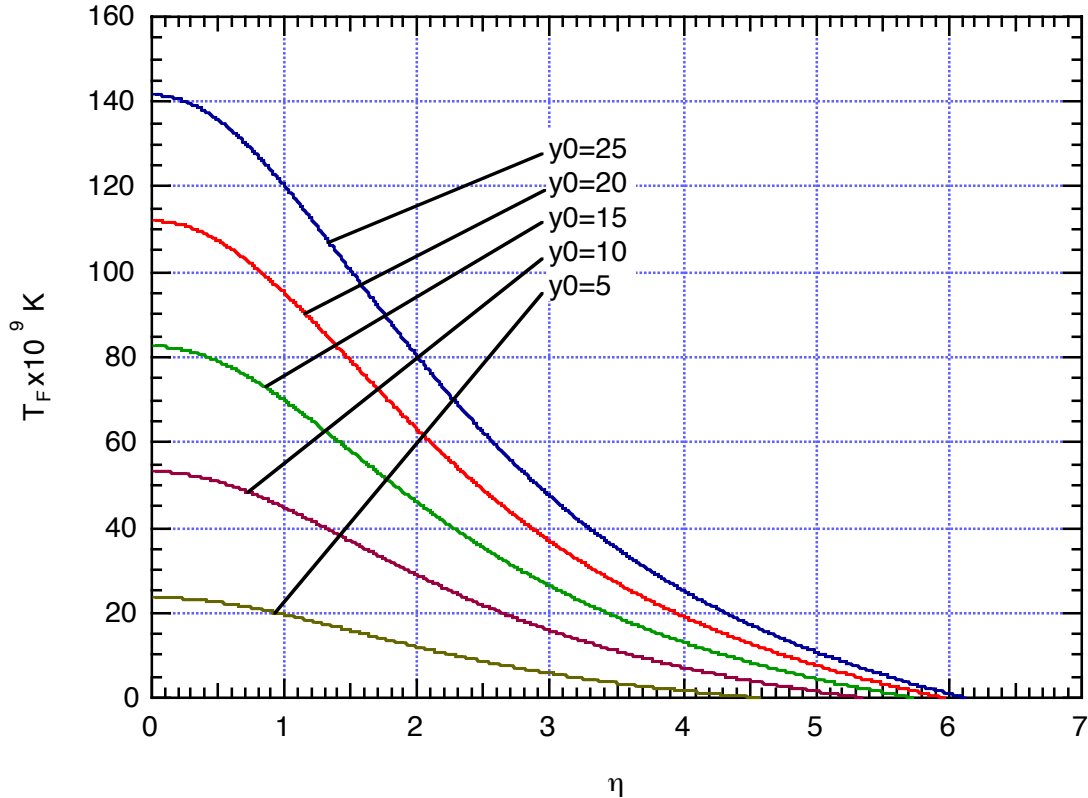


Fig. 6. The Fermi temperature in units of  $10^9$  K versus  $\eta$  for the following configurations:  $y_0 = 5, 10, 15, 20, 25$ : ( $M/M_C = .87, .953, .974, .983, .988$ ).

While the initial central temperature of a white dwarf star might be  $\approx 5 \cdot 10^8$  K the star cools over time through radiation from the surface, and also by neutrino losses. Hence, the zero temperature approximation is certainly a very good one for a sufficiently old quiescent white dwarf. Accretion from a binary companion will add a great deal of heat because accreted material (hydrogen and/or helium) releases additional gravitational energy; furthermore that material can undergo thermonuclear reactions at or near the surface, providing still more heat. However, we can see from Fig. 6 that for white dwarfs near the Chandrasekhar limit, the electron gas will still be highly degenerate so long as the core temperature is less than  $\approx 10^{10}$  K. This fact has important consequences, as we'll see in the next section.

### 3. Neutrinos and The Explosion Process

Neutrinos play a very important role in a Type Ia supernova explosion. We shall try to describe a few key points by simple arguments and order-of-magnitude estimates. Let's imagine that we have a very dense electron-degenerate white dwarf core consisting of equal parts of  $^{12}\text{C}$  and  $^{16}\text{O}$ . As we've seen in Fig. 6, the electron Fermi temperature will be very high. The density of the core will also be high, and it will be an increasing function of the total mass of the star. If thermonuclear reactions commence, they will add energy to the core, and heat it. At first this will occur at more or less constant density, so long as

the electrons remain highly degenerate and supply most of the pressure because, as we have seen, electron degeneracy pressure is largely independent of temperature. Energy is also stolen from the core by neutrino emission. There are several mechanisms by which neutrinos can be produced:

- a) The photo-neutrino process, in which a  $\bar{\nu}\nu$  pair replaces an outgoing photon in Compton scattering;
- b) The plasma process, in which a photon in the dense plasma acquires an effective mass and can thus decay via a virtual electron-positron pair to a  $\bar{\nu}\nu$  pair;
- c) The pair process, in which electron-positron pairs are produced from thermal radiation at very high temperatures, and decay to  $\bar{\nu}\nu$  pairs.
- d) The URCA process in which certain nuclei act as catalysts to transform electron energy into neutrino energy.

At the high densities and relatively low temperatures ( $T_9 \approx 1$ ) one initially has in the degenerate core, the plasma process is the most important, and serves as an efficient regulator to keep thermonuclear reactions from running away. This works as follows: The dense stellar plasma has the following dispersion relation between photon frequency  $\omega$  and wave number  $k$ :

$$\omega^2 = k^2 c^2 + \omega_0^2 \quad (3.1)$$

where  $\omega_0$  is the plasma frequency. In an ordinary non-degenerate ionized gas, the latter is given by the familiar formula:

$$\omega_0^2 = \frac{4\pi n_e e^2}{m_e} \quad (3.2)$$

In a degenerate electron gas one finds the following modification:

$$\omega_0^2 = \frac{4\pi e^2 n_e}{m_e} \left[ 1 + \left( \frac{\hbar}{m_e c} \right)^2 (3\pi^2 n_e)^{3/2} \right]^{-1/2} \quad (3.3)$$

Of course, in either case the effective mass of the photon is  $m = \frac{\hbar\omega_0}{c^2}$ . Now, at any fixed temperature, the plasma process neutrino emissivity first increases with density since  $m$  increases, providing more and more phase space for the outgoing pairs. However as the density increases the emissivity ultimately reaches a maximum and then decreases, because plasma modes require energy to be excited; thus when  $mc^2 > kT$ , the number of modes decreases as  $\exp(-mc^2/kT)$ . In Fig. 7, we plot the plasma neutrino emissivity versus density at the fixed temperature  $T=0.3 \cdot 10^9$  K.

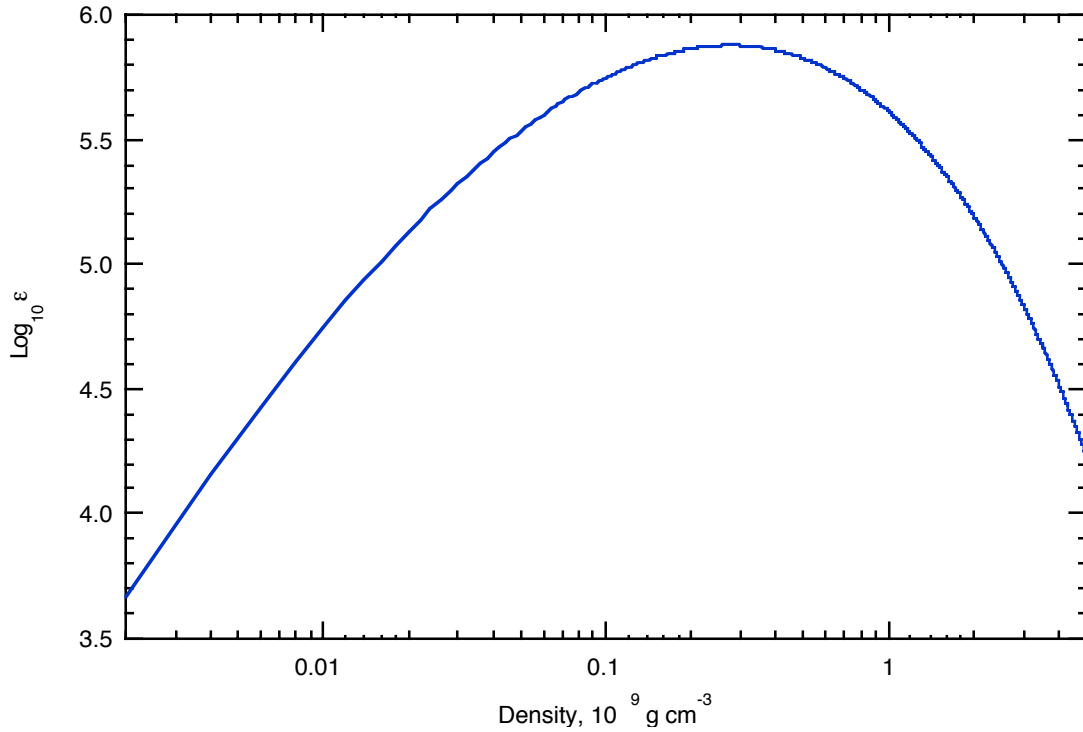
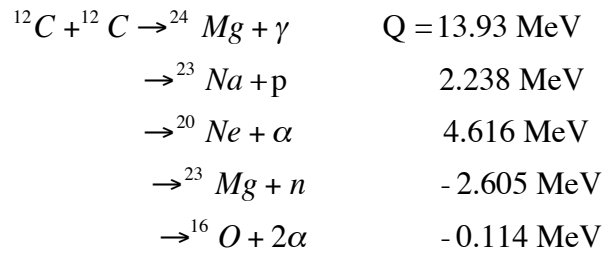


Fig.7 The plasma neutrino emission in ergs per gram per sec. is plotted versus the density for constant temperature  $T=0.3 \cdot 10^9$  K.

Now at any fixed density, the rate of any thermonuclear reaction is generally a sharply increasing function of the temperature. For example, consider the various reactions that can occur in the burning of  $^{12}\text{C}$ :



It can be shown that  $\epsilon(12-12)$ , the energy generated per gram per second in these reactions, is given by the following formula:

$$\epsilon = 1.27 \cdot 10^{43} X_{12}^2 \rho \frac{f}{T_9^{2/3}} \exp \left[ -84.17 \frac{(1 + .037 T_9^{1/3})}{T_9^{1/3}} \right] \quad (3.4)$$

where  $f$  is due to electron screening and is given by:

$$f = \exp \left[ 3.50 \frac{\rho_9^{1/3}}{T_9} \right]$$

while  $X_{12}$  is the fractional abundance of  $^{12}\text{C}$ . In Fig. 8 we plot  $\epsilon(12-12)$  and  $\epsilon(\text{Plasma})$  versus temperature for two different densities (expressed in units of  $10^9 \text{ g cm}^{-3}$ ):  $\rho_9=1$ , and  $\rho_9=2.0$ , in each case assuming  $X_{12}=0.5$ . It is easy to see that if  $\epsilon(12-12) < \epsilon(\text{Plasma})$ , the material will cool down. On the other hand, if  $\epsilon(12-12) > \epsilon(\text{Plasma})$ , the material will heat up. The point at which  $\epsilon(12-12) = \epsilon(\text{Plasma})$ , for each density, is labeled the “ignition point”; it is a point of unstable equilibrium. It is important to note that as we increase the density (by increasing the mass through accretion) the ignition point temperature actually decreases. This shows a principal reason why the supernova explosion can be initiated by accretion to a mass close to the Chandrasekhar limit.

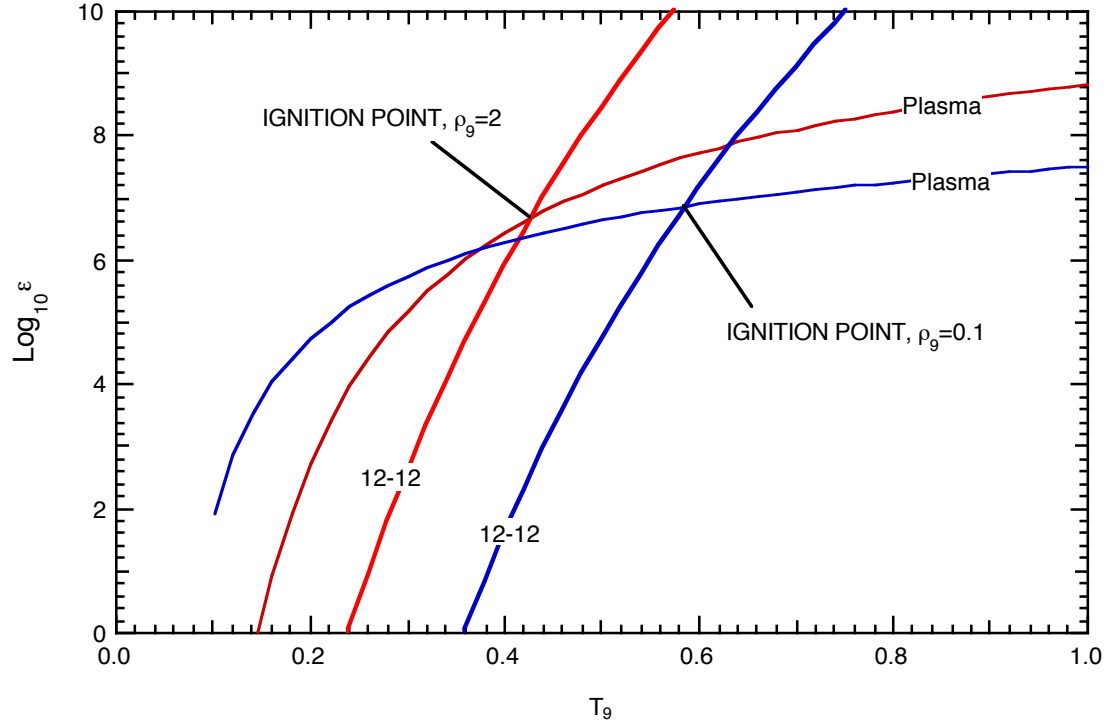


Fig.8  $\epsilon(12-12)$  and  $\epsilon(\text{Plasma})$  plotted as a function of temperature in units of  $10^9 \text{ K}$ , for two distinct densities. Red curves:  $\rho_9=2.0$ ; blue curves:  $\rho_9=0.1$ .

At higher temperatures the pair neutrino process is the most important. We shall now show that although the pair process energy loss rate increases rapidly with temperature, it is insufficient to prevent thermonuclear reactions from running away, since the thermonuclear energy generation rate increases much more rapidly. Let  $v$  be the relative velocity of electron and positron in a bath of high temperature thermal radiation, and let  $E$  be the sum of their energies. Then, from the standard electroweak model, we can show that:

$$\sigma \frac{v}{c} \approx 1.9 \cdot 10^{-45} \left( \frac{4E^2}{m_e^2 c^4} - 0.55 \right) \text{ cm}^2 \quad (3.5)$$



where  $\sigma$  is the weak interaction cross-section. The total energy loss per cubic centimeter per second,  $Q$ , arising from the pair process depends not only on  $\sigma v$  but also on the number densities of  $e^-$  and  $e^+$ :

$$Q_{pair} = \int (E_- + E_+) \sigma v dn_- dn_+ \quad (3.6)$$

To calculate the densities we once again employ Fermi-Dirac statistics. Assuming overall charge neutrality we have:

$$n_- = n_0 + n_+ = \frac{1}{\pi^2 \hbar^3} \int_0^\infty \frac{p^2 dp}{\exp\left[\frac{E - \mu_-}{kT}\right] + 1} \quad (3.7)$$

$$n_+ = \frac{1}{\pi^2 \hbar^3} \int_0^\infty \frac{p^2 dp}{\exp\left[\frac{E - \mu_+}{kT}\right] + 1}$$

where  $n_0$  is the number density of atomic electrons, while  $\mu_{+,-}$  are the chemical potentials of the positrons and electrons respectively. At sufficiently high temperatures,  $n_+ \gg n_0$  and we may ignore  $n_0$ . Then  $n_+ = n_-$ ; hence  $\mu_+ = \mu_-$ . However, if we assume equilibrium between electromagnetic pair production and annihilation:

$$n\gamma \leftrightarrow e^+ + e^-$$

then the chemical potentials must satisfy  $\mu_\gamma = \mu_+ + \mu_-$ . Since the chemical potential of thermal radiation is zero, we must then have  $\mu_+ = -\mu_-$  as well as  $\mu_+ = \mu_-$ . Consequently,  $\mu_+ = \mu_- = 0$ . Then,

$$n_+ = n_- = \frac{1}{\pi^2 \hbar^3} \int_0^\infty \frac{p^2 dp}{e^x + 1} \quad (3.8)$$

where  $x = E/kT = (p^2 c^2 + m_e^2 c^4)^{1/2} / kT$ . For  $kT \ll m_e c^2$  we can use the approximation:

$$\frac{1}{e^x + 1} \approx \exp\left(-\frac{m_e c^2}{kT}\right) \exp\left(-\frac{p^2}{2m_e kT}\right)$$

Then we obtain:

$$n_+ = n_- \approx \left(\frac{2m_e kT}{\pi \hbar^2}\right)^{3/2} \exp\left(-\frac{m_e c^2}{kT}\right) \quad (3.9)$$

For  $T \approx 10^9$  K, for example, this yields  $n_+ = n_- \approx 2 \cdot 10^{27} \text{ cm}^{-3}$ . Then employing (3.5) to obtain

$$\sigma v / c \approx 7 \cdot 10^{-45} \text{ cm}^2$$

and writing  $E_+ + E_- \approx 2m_e c^2$ , we find:

$$Q_{Pair} \approx n_+ n_- \sigma v (E_+ + E_-) \approx 10^{15} \text{ erg cm}^{-3} \text{ s}^{-1} \quad (3.10)$$

Although this estimate contains several rough approximations it is within an order of magnitude of the correct result at  $T=10^9$  K. The pair energy loss rate increases very rapidly with temperature. For  $kT \gg m_e c^2$  the integral in (3.8) may be approximated by:

$$\int_0^\infty \frac{p^2 dp}{e^x + 1} \approx \int_0^\infty \frac{p^2 dp}{e^{pc/kT} + 1} \approx 1.8 \left( \frac{kT}{c} \right)^3 \quad (3.11)$$

Therefore since  $\sigma v$  scales as  $E^2 \approx (kT)^2$ , we find that::

$$\begin{aligned} Q_{Pair} &\propto n_+ n_- \sigma v (E_+ + E_-) \\ &\propto (kT)^3 (kT)^3 (kT)^2 (kT) = (kT)^9 \end{aligned}$$

This crude estimate is also quite reliable: a more detailed calculation shows that  $Q_{Pair}$  increases by about 10 orders of magnitude between  $10^9$  and  $10^{10}$  K, to give:

$$Q_{Pair}(10^{10} \text{ K}) \approx 10^{25} \text{ erg cm}^{-3} \text{ s}^{-1} \quad (3.12)$$

At a density  $\rho=2 \cdot 10^9 \text{ g cm}^{-3}$  this corresponds to an energy loss rate of:

$$Q_{Pair}(10^{10} \text{ K}, 2 \cdot 10^9 \text{ g/cm}^3) \approx 5 \cdot 10^{14} \text{ erg g}^{-1} \text{ s}^{-1} \quad (3.13)$$

By comparison, the energy generation rate at the same temperature and density from  $\epsilon(12-12)$  is:

$$\epsilon(12-12) \approx 1 \cdot 10^{33} \text{ erg g}^{-1} \text{ s}^{-1} \quad (3.14)$$

## 4. A Simple Self-Similar Explosion Model

### 4.1 Formulation of the model

We shall now describe a very simple model of the explosion, first devised by F.J. Mayer and J.R. Reitz, and modified somewhat by EDC. It ignores almost all of the actual details, which are exceedingly complicated, but makes use only of the following essential assumptions:

- Spherical symmetry;
- Conservation of mass, expressed through the equation of continuity for the mass density;
- Conservation of momentum, expressed by Euler's equation of hydrodynamics ( this is just another form of Newton's second law);
- Conservation of energy.

- The explosion itself is characterized by only two parameters: the total energy it releases ( $\approx 10^{51-52}$  erg), and the time scale over which it does so ( $\approx 10-1000$  seconds).
- Two other energy releases are of comparable importance: the radioactive decays of  $^{56}\text{Ni}$  and  $^{56}\text{Co}$ . Here we ignore all the ugly details and characterize these simply by the amount of energy released (proportional to the mass of  $^{56}\text{Ni}$  produced in the explosion) and the time constants for the decays (9.5 days and 112 days for Ni and Co respectively.) Note that these times are larger by many orders of magnitude than the explosion time scale, a fact that yields an important simplification. We assume for simplicity that the initial distribution of the nickel is everywhere proportional to the mass density (although in fact we know that the nickel is concentrated in the core).
- To simplify our calculations further we shall also assume that once the explosion is ignited, radiation pressure so greatly dominates over gas pressure and degeneracy pressure that we can ignore the latter two pressures. In fact in a later section we shall justify this assumption by a simple calculation.
- Finally, even with all these simplifying assumptions, our problem is still too complex, because the equation of continuity, Euler's equation, and the energy conservation equation are coupled partial differential equations (in the variables  $r$  and  $t$ ). However, we can reduce them to ordinary differential equations by one further assumption: that the density and pressure evolve in time in a self-similar manner. This means, first of all, that there exists a time-dependent length scale:

$$r_s(t) = r_0 y(t) \quad (4.1)$$

where  $r_0 = r_s(t=0)$ , hence  $y(0)=1$ . Also, it means that the radial velocity of material at any point  $r$  and time  $t$  can be expressed as:

$$v = \frac{r}{r_s} \dot{r}_s = r \frac{\dot{y}}{y} \quad (4.2)$$

which implies that at any given time,  $v$  is proportional to  $r$ . Furthermore self-similarity requires the density to be expressed as:

$$\rho(r,t) = f\left(\frac{r}{r_s}\right) g(y)$$

In fact we shall assume that the function  $f$  is a simple Gaussian, although this is not an absolutely necessary requirement. Also, the equation of continuity requires that  $g(y)=1/y^3$ . So, let's begin by assuming that:

$$\rho(r,t) = \rho_0 \exp\left[-\left(\frac{r}{r_s}\right)^2\right] y^{-3} \quad (4.3)$$

and let's demonstrate explicitly that this satisfies the equation of continuity. The latter is:

$$\nabla \cdot (\rho \vec{v}) + \frac{\partial \rho}{\partial t} = 0$$

and when we have spherical symmetry it becomes

$$\frac{\partial(\rho v)}{\partial r} + \frac{2}{r}\rho v + \frac{\partial\rho}{\partial t} = 0 \quad (4.4)$$

Now, assuming that  $\rho$  is given by (4.3), we have:

$$\frac{\partial(\rho v)}{\partial r} = \frac{\partial}{\partial r} \left[ \frac{r\dot{y}}{y^4} \rho_0 \exp\left(-\left(\frac{r}{r_s}\right)^2\right) \right] = \frac{\dot{y}}{y} \rho - 2 \frac{r^2}{r_s^2} \frac{\dot{y}}{y} \rho$$

$$\frac{2}{r} \rho v = 2 \frac{\dot{y}}{y} \rho$$

$$\frac{\partial\rho}{\partial t} = \frac{2r^2}{r_s^3} \dot{r}_s \rho - \frac{3\dot{y}}{y} \rho = \frac{2r^2}{r_s^2} \frac{\dot{y}}{y} \rho - \frac{3\dot{y}}{y} \rho$$

Substituting these expressions into (4.4) we see that the equation of continuity is indeed satisfied. Next, let's consider Euler's equation:

$$\rho \frac{d\mathbf{v}}{dt} = -\frac{\partial p}{\partial r} - \frac{G\rho M(r)}{r^2} \quad (4.5)$$

which simply states that the mass per unit volume of a fluid times its acceleration (left hand side) is equal to the force per unit volume acting on the fluid (right hand side). That force per unit volume consists of two contributions: the pressure gradient, and the gravitational force per unit volume. In equilibrium, the left hand side vanishes, and (4.5) reduces to the familiar equation of hydrostatic equilibrium (2.9).

Now we must take into account that the time derivative of  $v$  has two contributions: the explicit derivative with respect to time at fixed position, and also the part which arises because  $v$  itself varies from one spatial location to another:

$$\begin{aligned} \rho \frac{d\mathbf{v}}{dt} &= \rho \left[ \frac{\partial \mathbf{v}}{\partial t} + \bar{\mathbf{v}} \cdot \nabla \mathbf{v} \right] \\ &= \rho \left[ \frac{\partial \mathbf{v}}{\partial t} + \mathbf{v} \frac{\partial \mathbf{v}}{\partial \mathbf{r}} \right] \end{aligned}$$

In the present case these two contributions reduce to the following expressions:

$$\frac{\partial \mathbf{v}}{\partial t} = r \frac{\ddot{y}}{y} - r \left( \frac{\dot{y}}{y} \right)^2$$

$$\mathbf{v} \frac{\partial \mathbf{v}}{\partial r} = r \left( \frac{\dot{y}}{y} \right)^2$$

Hence the left hand side of (4.5) is simply given by the formula:

$$\rho \frac{d\mathbf{v}}{dt} = \rho r \frac{\ddot{y}}{y} \quad (4.6)$$

Next let's consider the second term on the right hand side of (4.5): the gravitational force per unit volume. The mass interior to  $r$  is:

$$\begin{aligned}
 M(r) &= 4\pi \int_0^r r^2 \rho dr \\
 &= 4\pi \rho_0 y^{-3} \int_0^r r^2 \exp\left[-\left(\frac{r}{r_s}\right)^2\right] dr \\
 &= 4\pi \rho_0 r_0^3 \int_0^{r/r_s} u^2 e^{-u^2} du
 \end{aligned} \tag{4.7}$$

The total mass of the star  $M_0$  is obtained by taking the upper limit of the last integral in (4.7) to  $\infty$ :

$$M_0 = \pi^{3/2} \rho_0 r_0^3 \tag{4.8}$$

For finite  $r/r_s$  we expand the integrand of the last expression in a power series and integrate term by term:

$$\begin{aligned}
 \int_0^x \left[ u^2 - u^4 + \frac{1}{2!} u^6 - \frac{1}{3!} u^8 + \dots \right] du = \\
 \frac{x^3}{3} - \frac{x^5}{5} + \frac{x^7}{2 \cdot 7} - \dots
 \end{aligned}$$

For small  $x=r/r_s$  the leading term is sufficient and  $M(r)$  becomes:

$$M(r) \approx \frac{4\pi \rho_0}{3y^3} r^3 \tag{4.9}$$

In this case the gravitational force per unit volume becomes:

$$F_G \approx -\frac{4\pi G \rho_0}{3y^3} \rho r \tag{4.10}$$

Of course this expression is not exact; it is only valid for  $r \ll r_s$ . Nevertheless it can be shown that we make only a very small error in the final result if we employ (4.10) as if it were exact; hence we shall do this.

Finally let's consider the pressure gradient term in (4.5). Self-similarity requires the radial dependence of the pressure to be the same as that of the density:

$$P(r) = P(r=0) \frac{\rho y^3}{\rho_0} \tag{4.11}$$

Hence,

$$-\frac{\partial P}{\partial r} = \frac{2P(0)y}{\rho_0 r_0^2} \rho r \tag{4.12}$$

Now substituting (4.6), (4.10), and (4.12) in (4.5) we arrive at the following:

$$\rho r \frac{\ddot{y}}{y} = \rho r \frac{2P(0)y}{\rho_0 r_0^2} - \rho r \frac{4\pi G \rho_0}{3y^3}$$

We divide both sides by  $\rho r y$ , and transpose to find:

$$\frac{\ddot{y}}{y^2} + \frac{4\pi G \rho_0}{3y^4} = \frac{2P(r=0)}{\rho_0 r_0^2} \quad (4.13)$$

As mentioned earlier, we shall show that once the explosion starts, radiation pressure is dominant over gas and degeneracy pressure. Assuming tentatively that we can neglect the latter two pressures, and defining  $\Theta$  as the temperature at  $r=0$ , we can write:

$$P(r=0) = \frac{1}{3} a \Theta^4(t) \quad (4.14)$$

where  $a=7.6 \cdot 10^{-15}$  is the Stefan-Boltzmann constant in cgs. We also define a quantity  $\tau$  with the dimensions of time, by:

$$\tau^2 = \frac{3}{\sqrt{2\pi G \rho_0}} \quad (4.15)$$

Then (4.13) becomes our final form of Euler's equation:

$$\frac{\ddot{y}}{y^2} + \frac{4}{\sqrt{2\tau^2} y^4} = \frac{2a\Theta^4(t)}{3\rho_0 r_0^2} \quad (4.16)$$

Next we discuss conservation of energy. Let  $U$  be the total thermal energy of the star. Define  $E(t)$  as the energy generated in the explosion by thermonuclear reactions, and later by radioactive decay of  $^{56}\text{Ni}$  and  $^{56}\text{Co}$ . Also, define  $\Omega$  as the gravitational potential energy of the star, and  $L$  as the energy radiated from the surface of the star per second. Then conservation of energy is expressed by the equation:

$$\frac{dU}{dt} + P \frac{dV}{dt} + \frac{d\Omega}{dt} = \dot{E} - L \quad (4.17)$$

where the second term on the left hand side accounts for the work done by the stellar material and radiation in the expansion.

Of course (4.17) applies to the entire supernova, but we can write an analogous equation for each unit of mass as follows:

Let the thermal energy per unit volume be  $u$ . The assumption that radiation pressure greatly dominates over gas and degeneracy pressure is equivalent to assuming that the main contribution to  $u$  is the energy density of thermal radiation:

$$u = aT^4$$

In this case the thermal energy per unit mass is  $aT^4/\rho = a\Theta^4 y^3/\rho_0$ . Thus, from (4.16) we see that:

$$\frac{d}{dt} \left( \frac{u}{\rho} \right) = \frac{3}{2} r_0^2 \frac{d}{dt} \left[ y\ddot{y} + \frac{4}{\sqrt{2}\tau^2} \frac{1}{y} \right] \quad (4.18)$$

The volume per unit mass is  $1/\rho$ . Hence, the rate at which work is done per unit mass by the supernova “fluid” is:

$$\begin{aligned} P \frac{d}{dt} \left( \frac{1}{\rho} \right) &= - \frac{P}{\rho^2} \frac{d\rho}{dt} \\ &= - \frac{P}{\rho^2} \left( \frac{\partial \rho}{\partial t} + v \frac{\partial \rho}{\partial r} \right) \\ &= \frac{3P}{\rho} \frac{\dot{y}}{y} \\ &= \frac{3}{2} r_0^2 \frac{\dot{y}}{y} \left[ y\ddot{y} + \frac{4}{\sqrt{2}\tau^2} \frac{1}{y} \right] \end{aligned} \quad (4.19)$$

The gravitational energy per unit mass is:

$$\begin{aligned} \frac{\Omega}{M_0} &= - \frac{G}{M_0} \int \frac{M(r) dM(r)}{r} \\ &= - (4\pi)^2 \frac{G}{M_0} \int_0^\infty r \rho(r) dr \int_0^r r'^2 \rho(r') dr' \\ &= - \frac{1}{\sqrt{2\pi}} \frac{GM_0}{yr_0} \end{aligned} \quad (4.20)$$

Hence,

$$\frac{d}{dt} \left( \frac{\Omega}{M_0} \right) = \frac{3}{2} r_0^2 \left[ \frac{2GM_0}{3\sqrt{2\pi}r_0^3} \right] \frac{\dot{y}}{y^2} \quad (4.21)$$

We can construct an energy conservation equation for each unit of mass, analogous to (4.17) as follows:

$$\frac{d}{dt} \left[ \frac{u}{\rho} \right] + P \frac{d}{dt} \left[ \frac{1}{\rho} \right] + \frac{d}{dt} \left[ \frac{\Omega}{M_0} \right] = \frac{1}{M_0} (\dot{E} - L) \quad (4.22)$$

Substituting (4.18), (4.19), and (4.21) into the left hand side of (4.22), combining terms, and making use of (4.8) and (4.15), we arrive at:

$$\frac{d}{dt} \left[ y\ddot{y} + \frac{1}{2}\dot{y}^2 - \frac{1}{\tau^2 y} \right] = \frac{2}{3M_0 r_0^2} [\dot{E} - L] \quad (4.23)$$

We can integrate both sides of (4.23) immediately:

$$y\ddot{y} + \frac{1}{2}\dot{y}^2 - \frac{1}{\tau^2 y} = \frac{2}{3M_0 r_0^2} \left[ E - \int L dt \right] + C$$

where C is a constant of integration. Now at t=0, before the expansion starts, E=0. Also  $\dot{y}(0) = 0$ , since the velocity of expansion at t=0 is still zero. Furthermore at t=0 we still have hydrostatic equilibrium, so  $\ddot{y}(0) = 0$  (recall (4.6)). Since y(0)=1, we then have C=1/τ<sup>2</sup>; hence:

$$y\ddot{y} + \frac{1}{2}\dot{y}^2 + \frac{1}{\tau^2} \left( 1 - \frac{1}{y} \right) = \frac{2}{3M_0 r_0^2} \left[ E - \int_0^t L dt' \right] \quad (4.24)$$

At this point it is convenient to introduce a dimensionless variable z, defined by t=τz.

Also, defining the symbols:  $y' \equiv \frac{dy}{dz}$ ,  $y'' \equiv \frac{d^2 y}{dz^2}$ , we rewrite (4.24) as follows:

$$yy'' + \frac{1}{2}y'^2 + \left( 1 - \frac{1}{y} \right) = \frac{2\tau^2}{3M_0 r_0^2} \left[ E - \tau \int_0^{z/\tau} L dz' \right] \quad (4.25)$$

Now,  $\frac{2\tau^2}{3M_0 r_0^2} = \frac{\sqrt{2\pi} r_0}{GM_0^2} = \frac{1}{|\Omega_0|}$ , where  $\Omega_0$  is the gravitational potential energy at time t=0.

Thus our energy conservation equation becomes:

$$yy'' + \frac{1}{2}y'^2 + \left( 1 - \frac{1}{y} \right) = \frac{1}{|\Omega_0|} \left[ E - \tau \int_0^{z/\tau} L dz' \right] \quad (4.26)$$

Next, let's discuss E. As already mentioned, we can separate E into two parts:

$$E = E_E + E_R$$



where  $E_E$  is the energy generated by the thermonuclear reactions contributing to the explosion, and  $E_R$  is energy generated by the radioactive decay. We can model  $E_E$  as follows:

$$E_E = q|\Omega_0| \left[ 1 - \exp\left(-\frac{t}{t_1}\right) \right] \quad (4.27)$$

The motivation for (4.27) is as follows:  $|\Omega_0|$  is a convenient unit of energy, and  $q$  is a numerical factor that expresses the explosion strength in terms of this unit. We shall see that the choice  $q \approx 1.5$  yields reasonable Type Ia light curves. The quantity in square brackets is simply a convenient smooth function that starts at zero at  $t=0$  and turns on in a time of the order of  $t_1$ . We shall see that the value of  $t_1$  is not very critical; anything in the range 10-1000 seconds will serve.

Next let us consider  $E_R$ . First we note some facts from nuclear physics:  $^{56}\text{Ni}$  decays to  $^{56}\text{Co}$  with the emission of several gamma rays, the total energy of which is  $Q_2 = 1.73$  MeV. The mean life for  $^{56}\text{Ni}$  decay is:  $\tau_2 = \frac{1}{\lambda_2} = 7.6 \cdot 10^5$  sec.  $^{56}\text{Co}$  decays to  $^{56}\text{Fe}$  by many gamma rays with a total energy release of  $Q_3 = 3.68$  MeV. The mean life for  $^{56}\text{Co}$  decay is:  $\tau_3 = \frac{1}{\lambda_3} = 9.8 \cdot 10^6$  sec. Now let's set up some elementary equations to describe the decay chain. The rate of  $^{56}\text{Ni}$  decay is:

$$R_N = \lambda_2 N_0 \exp(-\lambda_2 t) \quad (4.28)$$

where  $N_0$  is the initial number of  $^{56}\text{Ni}$  nuclei. Let  $N_3(t)$  be the number of  $^{56}\text{Co}$  nuclei. It satisfies the equation:

$$\frac{dN_3}{dt} = -\lambda_3 N_3 + \lambda_2 N_0 \exp(-\lambda_2 t) \quad (4.29)$$

where the first term on the RHS describes the decay of cobalt, while the second describes the population of cobalt by nickel decay. The solution to this equation satisfying the initial condition  $N_3=0$  is:

$$N_3 = \frac{\lambda_2}{\lambda_2 - \lambda_3} N_0 \left[ \exp(-\lambda_3 t) - \exp(-\lambda_2 t) \right] \quad (4.30)$$

The rate of  $^{56}\text{Co}$  decay is thus:

$$R_C = \frac{\lambda_2 \lambda_3}{\lambda_2 - \lambda_3} N_0 \left[ \exp(-\lambda_3 t) - \exp(-\lambda_2 t) \right] \quad (4.31)$$

Hence the rate of energy release from the decay chain is:

$$\begin{aligned}\frac{dE_R}{dt} &= Q_2 R_N + Q_3 R_C \\ &= N_0 Q_2 \lambda_2 \exp(-\lambda_2 t) + N_0 Q_3 \frac{\lambda_2 \lambda_3}{\lambda_2 - \lambda_3} [\exp(-\lambda_3 t) - \exp(-\lambda_2 t)]\end{aligned}\quad (4.32)$$

The total radioactive decay energy released between time 0 and t is obtained by integrating both sides of (4.32):

$$\begin{aligned}E_R &= N_0 Q_2 (1 - \exp(-\lambda_2 t)) + N_0 Q_3 \frac{\lambda_2}{\lambda_2 - \lambda_3} (1 - \exp(-\lambda_3 t)) - N_0 Q_3 \frac{\lambda_3}{\lambda_2 - \lambda_3} (1 - \exp(-\lambda_2 t)) \\ &= N_0 \left[ Q_2 + Q_3 - (Q_2 - Q_3 \frac{\lambda_3}{\lambda_2 - \lambda_3}) \exp(-\lambda_2 t) - Q_3 \frac{\lambda_2}{\lambda_2 - \lambda_3} \exp(-\lambda_3 t) \right]\end{aligned}$$

Inserting numerical values in this last equation we obtain:

$$E_R = (5.41 \text{ MeV}) \cdot N_0 [1 - .26 \exp(-\lambda_2 t) - .74 \exp(-\lambda_3 t)] \quad (4.33)$$

Next we want to express  $N_0$  in terms of the mass of  $^{56}\text{Ni}$  created in the explosion. Let  $f$  be the fraction of a solar mass of nickel so created. Then,

$$N_0 = f \frac{2 \cdot 10^{33} \text{ g}}{56 m_p} = 2.1 \cdot 10^{55} f$$

where  $m_p = 1.67 \cdot 10^{-24} \text{ g}$  is the proton mass. Thus (4.33) becomes:

$$E_R = 1.8 \cdot 10^{50} f [1 - .26 \exp(-\lambda_2 t) - .74 \exp(-\lambda_3 t)] \text{ ergs} \quad (4.34)$$

Since  $1.8 \cdot 10^{50} \text{ ergs}$  is within an order of magnitude or so of  $q|\Omega_0|$ , it's convenient to define the dimensionless quantity

$$\delta = \frac{1.8 \cdot 10^{50} f \text{ erg}}{q|\Omega_0| \text{ erg}} \quad (4.35)$$

Then, putting all this together, we have:

$$\frac{E}{|\Omega_0|} = q [1 - \exp(-\lambda_1 t) + \delta (1 - .26 \exp(-\lambda_2 t) - .74 \exp(-\lambda_3 t))] \quad (4.36)$$

Recall that  $\lambda_1 = 1/\tau_1 \approx .1$  to  $.001$ , while  $\lambda_2 = 1.31 \cdot 10^{-6}$  and  $\lambda_3 = 1.02 \cdot 10^{-7}$  (all in  $\text{sec}^{-1}$ ). Also note that for numerical integration of (4.26) it is convenient to make use of the dimensionless variables  $z = t/\tau$  and  $\beta_{1,2,3} = \tau \lambda_{1,2,3}$  in (4.36).

## 4.2 The temperature

Let's now recall eq'ns (4.15) and (4.16):

$$\frac{\ddot{y}}{y^2} + \frac{4}{\sqrt{2}\tau^2 y^4} = \frac{2a\Theta^4(t)}{3\rho_0 r_0^2} \quad (4.16)$$

$$\tau^2 = \frac{3}{\sqrt{2}\pi G \rho_0} \quad (4.15)$$

Making the change of variable  $t=\tau z$  in (4.16), and substituting (4.15) in (4.16) we obtain:

$$\Theta^4(z) = \frac{\pi G \rho_0^2 r_0^2}{\sqrt{2}a} \left[ \frac{y''}{y^2} + \frac{4}{\sqrt{2}} \frac{1}{y^4} \right] \quad (4.37)$$

Initially  $y=1$  and  $y''=0$ . Thus:

$$\Theta(0) = \left[ \frac{2\pi G \rho_0^2 r_0^2}{a} \right]^{1/4} \quad (4.38)$$

The quantities  $\rho_0$  and  $r_0$  cannot be chosen independently, because  $M_0 = \pi^{3/2} \rho_0 r_0^3$  is fixed at 1.4 solar masses  $= 2.8 \cdot 10^{33}$  g. Substituting  $r_0^2 = \frac{M_0^{2/3}}{\pi \rho_0^{2/3}}$  in (4.38), we obtain:

$$\Theta(0) = 2.44 \cdot 10^7 \rho_0^{1/3} \text{ deg K} \quad (4.39)$$

as well as:

$$r_0 = 7.95 \cdot 10^{10} \rho_0^{-1/3} \text{ cm} \quad (4.40)$$

where in each case  $\rho_0$  is in grams/cm<sup>3</sup>. For convenience  $\Theta(0)$  and  $r_0$  are plotted versus  $\rho_0$  in Fig 10.

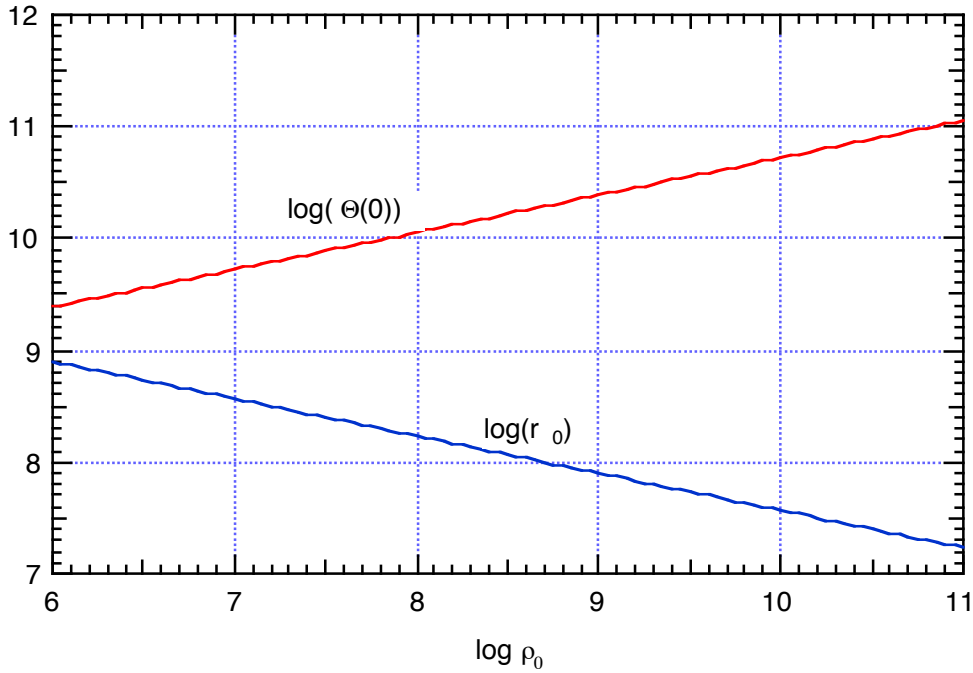


Fig. 10.

Referring back to Fig. 2 we see that when  $M \approx .98-.99 M_C$ ,  $\rho_0 \approx 3 \cdot 10^9$  g/cm<sup>3</sup>, in which case (4.39) and (4.40) yield:

$$\Theta(0)=3.5 \cdot 10^{10} \text{ K} \quad (4.41)$$

$$r_0 = 5.5 \cdot 10^7 \text{ cm} \quad (4.42)$$

Assuming (4.41), the radiation pressure at the origin and at  $t=0$  is

$$P_{Rad} = \frac{a}{3} [\Theta(0)]^4 = 3.8 \cdot 10^{27} \text{ dynes / cm}^2 \quad (4.43)$$

Meanwhile in the zero-temperature approximation, valid if  $T_F \gg T$ , the degeneracy pressure is given by (2.23) with (2.24), where  $x=0.00799\rho^{1/3} = 11.5$  assuming  $\mu_e=2$ . Thus we find:

$$P_{degen} = 2.1 \cdot 10^{27} \text{ dynes / cm}^2 \quad (4.44)$$

The gas pressure is  $P_{Gas}=nk\Theta$  where  $n$  is the total number of particles including electrons as well as nuclei. Since all the electrons may be assumed ionized at this high temperature,

$$nk\Theta \approx \frac{\rho}{2m_p} k\Theta = 4.3 \cdot 10^{27} \text{ dynes / cm}^2 \quad (4.45)$$

Eq'ns (4.43)-(4.45) indicate that all 3 pressures are comparable at the origin and at  $t=0$ . However, as time elapses and  $y$  increases very rapidly,  $P_{Rad} \propto 1/y^3$ , while  $P_{degen} \propto 1/y^4$  so long as the electrons are relativistic but then is proportional to  $1/y^5$  in the non-relativistic regime; meanwhile the gas pressure is proportional to  $y$  to the minus 15/4 power. Thus for all practical purposes, we are safe in ignoring the degeneracy and gas pressures.

### 4.3 Preliminary study of the differential equation

Now let's return to our basic differential equation:

$$yy'' + \frac{1}{2}y'^2 + \left(1 - \frac{1}{y}\right) = \frac{1}{|\Omega_0|} \left[ E - \tau \int_0^{t/\tau} Ldz' \right] \quad (4.46)$$

We have not yet discussed the second term on the right hand side, which represents the energy loss due to luminosity. This is actually a thorny problem, because we cannot determine the luminosity until we have some understanding of the opacity of the supernova envelope. We shall thus postpone a discussion of opacity and luminosity, and first deal with the simpler problem of getting a general grasp of the behavior of the function  $y$  at fairly early times, when the luminosity loss is negligible. To make our problem still simpler we shall also ignore the radioactive decays for the moment, and include only the explosion contribution to  $E$ . In this case (4.46) reduces to the equation:

$$yy'' + \frac{1}{2}y'^2 + \left(1 - \frac{1}{y}\right) = q(1 - e^{-\beta_1 z}) \quad (4.47)$$

with the boundary conditions  $y(0)=1$ ,  $y'(0)=0$ ,  $y''(0)=0$ . Also we recall that:

$$\tau^2 = \frac{3}{\sqrt{2\pi G\rho_0}}$$

Choosing  $\rho_0=3\cdot 10^9$  g/cm<sup>3</sup> we find  $\tau=.058$  sec. Thus for example, if we choose  $t_1=100$  sec, we have:

$$\beta_1=.00058$$

Equation (4.47) can be integrated numerically in a straightforward manner using a 4<sup>th</sup> order Runge-Kutta technique. In what follows we shall present some results from this integration program. First, choosing  $q=1.5$  we plot  $\dot{y}$  versus time  $t$  for  $t_1=30, 100, 300,$  and  $1000$  sec in Fig. 11. Note that for sufficiently long times,  $\dot{y}$  reaches a positive asymptotic value. This can easily be understood from (4.47) as follows. For  $t \gg t_1$  the right hand side approaches  $q$ . Now if  $q > 1$ , we can expect that  $1/y$  and  $yy''$  will both go to zero. Hence

$$y' \rightarrow \sqrt{2(q-1)} = 1 \quad \text{for } q = 1.5$$

and therefore  $\dot{y} = \tau^{-1}y' \rightarrow 17.24$ .

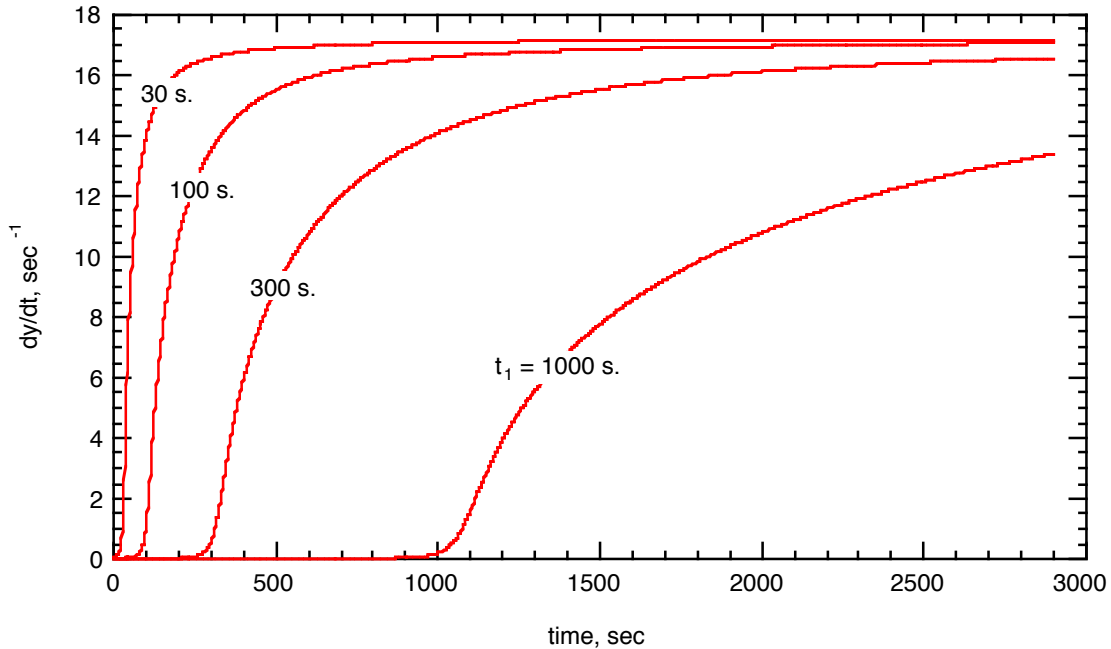


Fig. 11  $dy/dt$  versus  $t$  for various choices of  $t_1$ . In each case,  $q=1.5$ .

Next using (4.37) we plot the central temperature in deg K versus time for the same conditions. Note that the central temperature always decreases with time if  $q > 1$ .

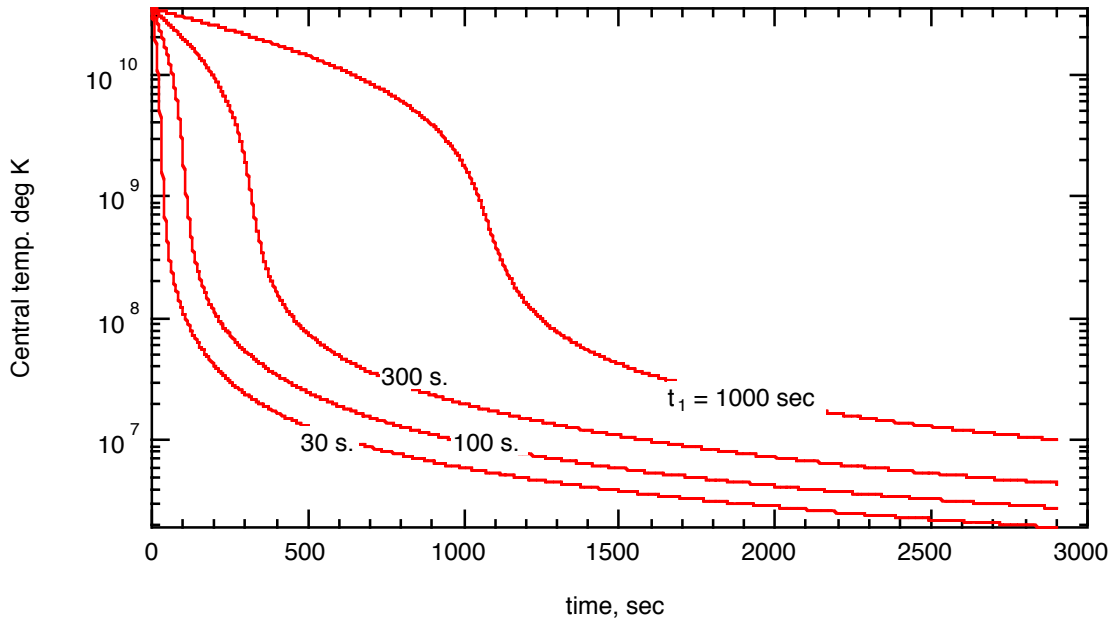


Fig. 12 Central temperature versus  $t$  for various choices of  $t_1$ . In each case,  $q=1.5$ .

For  $q>1$ ,  $y$  keeps increasing for all  $t$ . When  $q=1$ ,  $dy/dt \rightarrow 0$  at  $t \rightarrow \infty$ . However, for  $q<1$ ,  $dy/dt$  reaches zero at a finite time  $t$ , and remains at zero as  $t$  increases. This is shown in Fig.13. In fact the results obtained for  $q<1$  can also be understood intuitively from examination of (4.47). In the limit of large  $t$ , when  $y'=y''=0$ , we have  $y=(1-q)^{-1}$ .

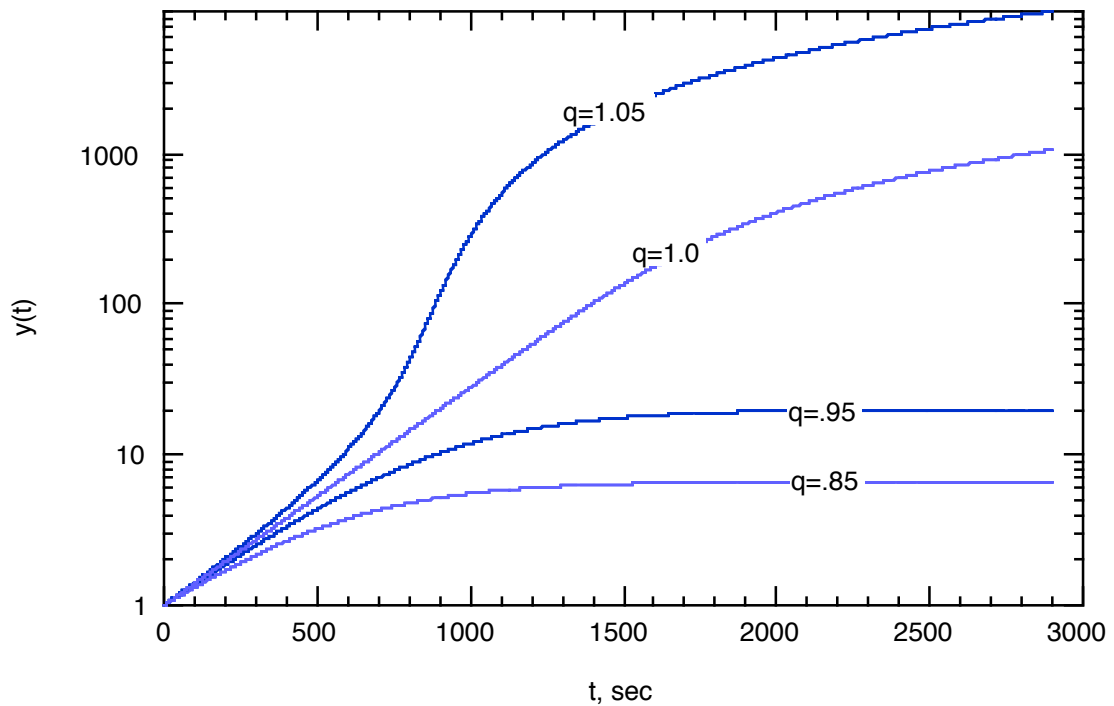


Fig. 13  $y(t)$  versus  $t$  for various values of  $q$ . In all cases,  $t_1=300$  sec.

#### 4.4 Opacity in First Approximation

Returning to the case  $q=1.5$  where the gas continues to expand rapidly, let's plot the central density and the central temperature versus time for the first day (see Fig.14). The figure reveals that the central temperature after 1 day is about  $10^5$  deg K, while the central density is about  $10^{-9}$  g/cm<sup>3</sup>. At this time, which is many orders of magnitude greater than  $t_1$  the expansion is uniform to an excellent approximation (and this is not significantly altered by inclusion of radioactive decay energy and luminosity loss). Let's inquire about the opacity of the material given such temperatures and densities. In an ordinary static plasma there are 4 processes that contribute to the opacity: free-free transitions, bound-free transitions, bound-bound transitions, and electron scattering. If we were to consult the opacity tables and formulae, we would find that for a *static* plasma at  $10^5$  K and  $10^{-9}$  g/cm<sup>3</sup> consisting mainly of nickel/cobalt and silicon, the first three processes contribute very little compared to electron scattering. As for the latter, we can estimate it, because we know the Thompson scattering cross-section of low-energy photons by free electrons:

$$\sigma_T = \frac{8\pi}{3} \frac{e^4}{m_e^2 c^4} = 6.6 \cdot 10^{-25} \text{ cm}^2 \quad (4.48)$$

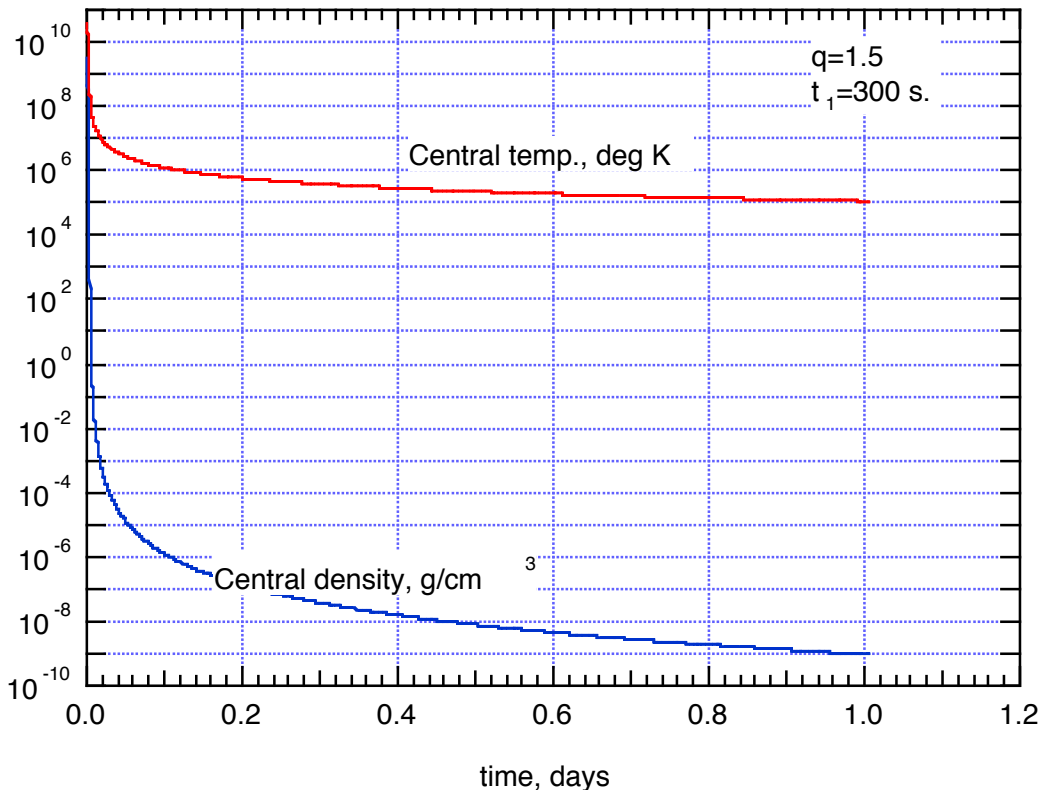


Fig. 14 Central density and central temperature vs. time for  $q=1.5$ ,  $t_1=300$  s.

The electron scattering opacity is then

$$\begin{aligned} \kappa_e &= \sigma_T \frac{n_e}{\rho} \\ &= \sigma_T \frac{1}{\mu_e m_p} = \frac{.39}{\mu_e} \text{ cm}^2 / \text{gm} \end{aligned} \quad (4.49)$$

Here,  $1/\mu_e$  is the number of free electrons per nucleon. At a temperature of  $10^5$  K where nickel or cobalt and silicon are at most triply ionized if in thermal equilibrium,  $1/\mu_e$  might be of the order of 0.1; hence we might expect  $\kappa_e \approx 0.02\text{-}0.04$   $\text{cm}^2/\text{gm}$ .

However, our plasma is **not** static; on the contrary it is expanding uniformly and radially with a velocity proportional to the distance from the origin. Then, consider Fig. 15, which shows a photon emitted at time  $t$  from an atom at point P at a distance  $r$  from the origin O. The photon travels a distance  $R$  and is absorbed by an atom at point Q at time  $t' = t + \Delta t = t + R/c$ , at a distance  $r'$  from the origin. The atom at P had velocity  $\mathbf{v} = \mathbf{r}/t$ ; the atom at Q has velocity  $\mathbf{v}' = \mathbf{r}'/t'$ . If the photon had frequency  $\nu_0$  in the rest frame of P, then in the rest frame of Q it has frequency:



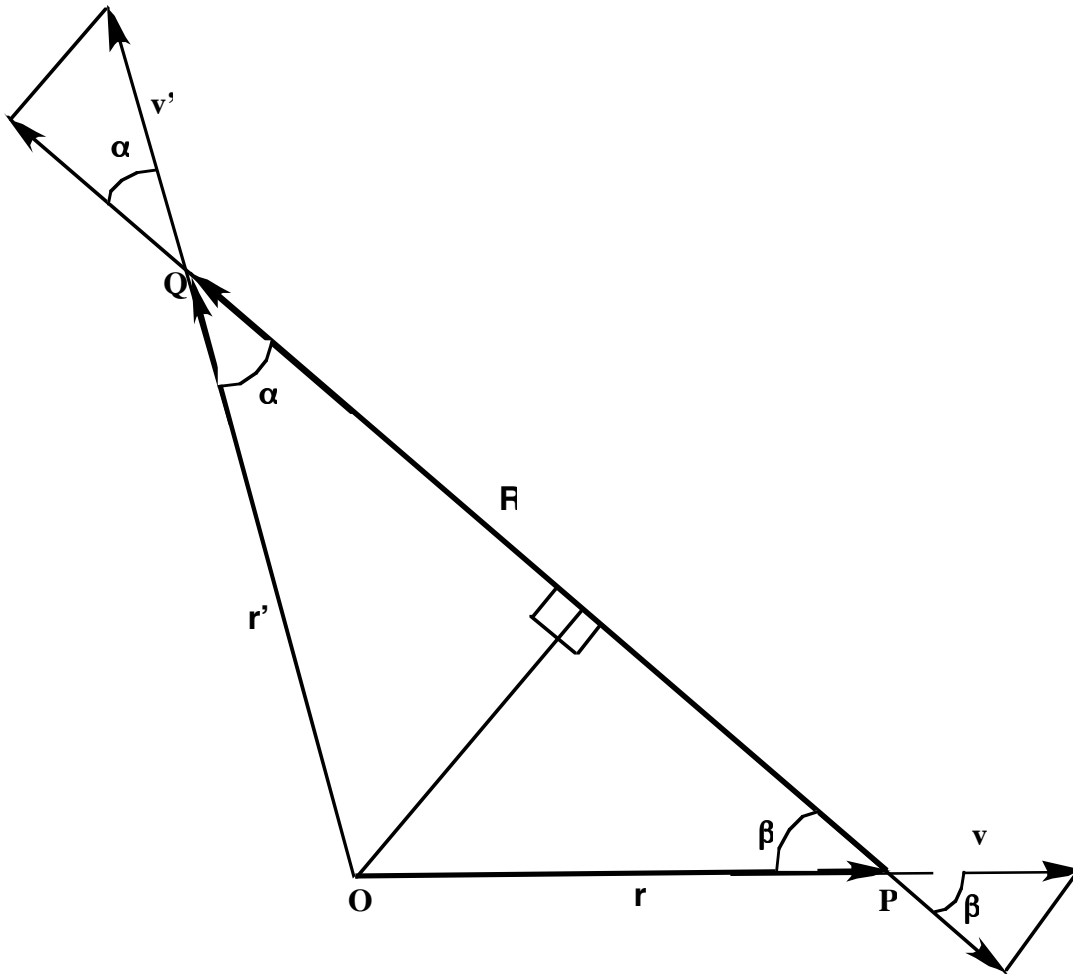


Fig. 15

$$\begin{aligned}
 v &= v_0 \left[ 1 - \frac{1}{c} (v' \cos \alpha + v \cos \beta) \right] \\
 &= v_0 \left[ 1 - \frac{1}{c} \left( \frac{r'}{t'} \cos \alpha + \frac{r}{t} \cos \beta \right) \right]
 \end{aligned}
 \tag{4.50}$$

Now  $\frac{r'}{t'} = \frac{r'}{t \left( 1 + \frac{R}{ct} \right)} \approx \frac{r'}{t} - \frac{r' R}{ct^2}$ ; hence:

$$\begin{aligned}
 \frac{v - v_0}{v_0} &= -\frac{1}{ct} (r' \cos \alpha + r \cos \beta) + \frac{r' R}{c^2 t^2} \\
 &= -\frac{R}{ct} + \frac{R r'}{ct ct} \approx -\frac{R}{ct} = -\frac{\Delta t}{t}
 \end{aligned}
 \tag{4.51}$$

It's interesting to note that that the fractional Doppler shift is independent of the direction of the photon and its point of origin, but depends only on the time at which it was emitted and the time interval over which it traveled before being absorbed!

Suppose that  $\nu_0$  is slightly higher than the resonance frequency of a bound-bound transition. Then the photon will travel until its frequency is Doppler shifted downward into the resonance frequency band, where it has a relatively high probability of being absorbed. If there are very many weak bound-bound transitions in the plasma (and this will be the case for our nickel /cobalt- silicon plasma) then the opacity should be considerably enhanced by this mechanism compared to that for pure electron scattering. Actual calculation of the enhancement is far from elementary, however, and involves many uncertainties, mainly due to our ignorance of the thousands of atomic oscillator strengths involved. We can only guess that the enhancement might be at least an order of magnitude, hence that the opacity might be as large as .5 or 1 cm<sup>2</sup>/gm. In the naïve model calculation that follows we shall thus assume that  $\kappa$  is in the range .02 to 1 cm<sup>2</sup>/g and independent of temperature and density.

#### 4.5 Luminosity in the First Approximation

The luminosity of the supernova is related to the effective temperature  $T_{\text{eff}}$  and radius  $R_p$  of the photosphere by the formula:

$$L = 4\pi R_p^2 \sigma T_{\text{eff}}^4 \quad (4.52)$$

where  $\sigma = 5.67 \cdot 10^{-5}$  erg cm<sup>-2</sup> s<sup>-1</sup> deg K<sup>-4</sup> is the Stefan-Boltzmann constant. Here  $T_{\text{eff}}$  is the temperature at  $R_p$ . Of course the main problem is to determine  $R_p$ . We shall define it as the radius where the optical depth of a radial ray from  $r = \infty$  is equal to unity:

$$\tau = 1 = \int_{R_p}^{\infty} \kappa \rho dr \quad (4.53)$$

According to the Gaussian model this is:

$$\begin{aligned} 1 &= \rho_0 y^{-3} \kappa \int_{R_p}^{\infty} \exp\left[-\left(\frac{r}{r_s}\right)^2\right] dr \\ &= \rho_0 y^{-3} \kappa r_s \int_w^{\infty} \exp(-u^2) du \end{aligned} \quad (4.54)$$

where  $w = R_p/r_s$ . Eq'n (4.54) can be rewritten as:

$$\frac{y^2 \sqrt{\pi}}{2\rho_0 r_0 \kappa} = 1 - \text{erf}(w) \quad (4.55)$$

where erf is the error function. Now, according to the NBS Handbook of Mathematical Functions (ed. M. Abramowitz and I. Stegun), formula 7.1.27, p. 299, the following is a very good approximation to  $1-\text{erf}(w)$ :

$$1 - \text{erf}(w) \cong \frac{1}{\left[1 + a_1 w + a_2 w^2 + a_3 w^3 + a_4 w^4\right]^4} \quad (4.56)$$

where:

$$a_1 = .278393$$

$$a_2 = .230389$$

$$a_3 = .000972$$

$$a_4 = .078108$$

Substituting (4.56) in (4.55) we have:

$$1 + a_1 w + a_2 w^2 + a_3 w^3 + a_4 w^4 = \left[ \frac{2\kappa\rho_0 r_0}{\pi^{1/2}} \right]^{1/4} \frac{1}{y^{1/2}} \quad (4.57)$$

Finally we substitute eq'n (4.40):

$$r_0 = 7.95 \cdot 10^{10} \rho_0^{-1/3} \quad (4.40)$$

in (4.57) to obtain:

$$1 + a_1 w + a_2 w^2 + a_3 w^3 + a_4 w^4 = 547 \frac{\kappa^{-1/4} \rho_0^{1/6}}{y^{1/2}} \quad (4.58)$$

In Fig. 16 we plot  $w$  versus  $y$  for typical conditions.

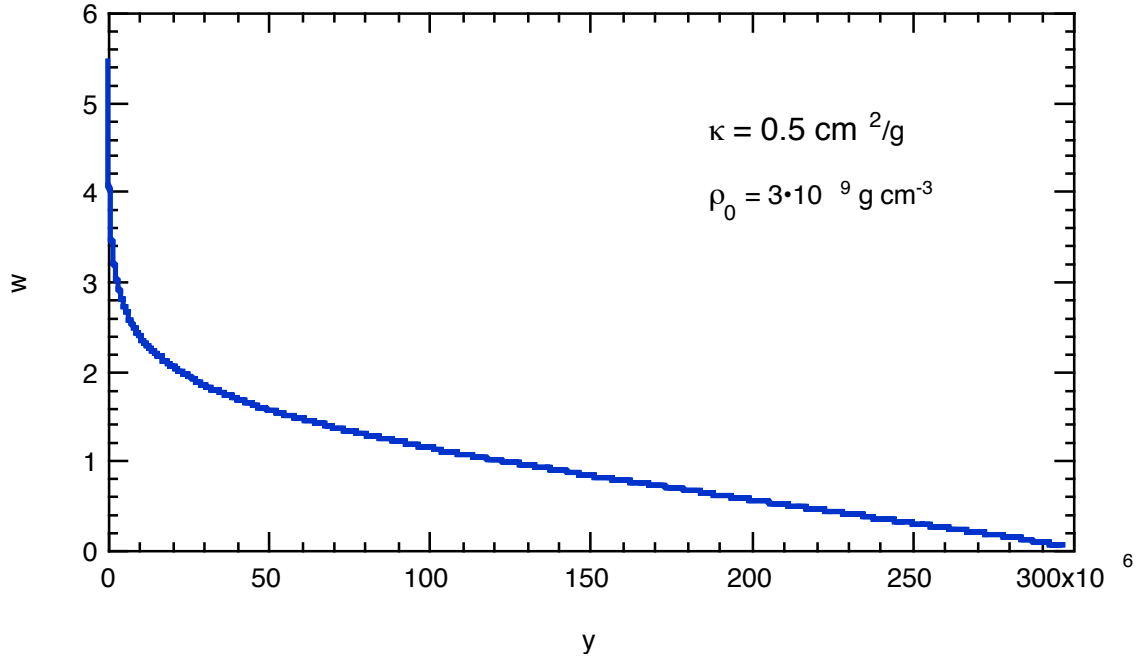


Fig. 16 A plot of  $w$  versus  $y$  for typical conditions

For the purpose of numerical computation it is useful to fit the family of curves, of which Fig. 16 is one example, by a single analytical expression. We find that

$$w = a + b \cdot \exp(-cy) + d \cdot \exp(-ey) \quad (4.59)$$

yields a good fit with the parameters:

$$a = -.767$$

$$b = 2.89$$

$$c = 2.89 \cdot 10^{-9} \kappa^F \left( \frac{\rho_0}{3 \cdot 10^9} \right)^G \quad (4.60)$$

$$d = 1.761$$

$$e = 1.229 \cdot 10^{-7} \kappa^F \left( \frac{\rho_0}{3 \cdot 10^9} \right)^G$$

$$F = -.48, G = -.32$$

Fig 17. shows a plot of the radius of the photosphere  $R_p = r_0 y w$  as a function of  $y$ . Recall that  $y$  is very nearly linear in  $t$  for  $t \gg t_1$ . Thus we see from Fig. 17 for given opacity and  $\rho_0$  that  $R_p$  reaches a maximum at a certain time and then decreases. Of course we cannot determine that time until we solve the complete equation (4.46) including the radioactivity contribution and the luminosity loss term.

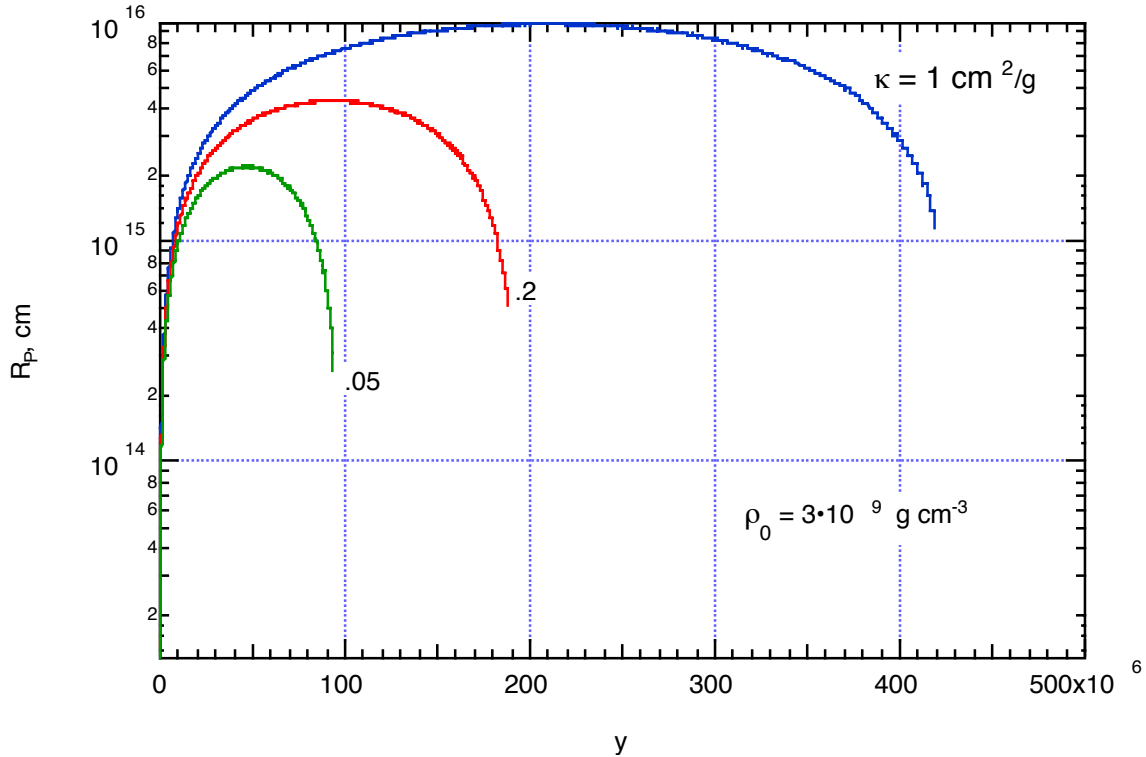


Fig. 17 Plots of  $R_p$  vs.  $y$  for typical opacity and density values.

We must take into account one more detail before using the self-similar model to calculate supernova Ia light curves. As time progresses and the photosphere retreats it eventually renders transparent more and more of the radioactive nickel and cobalt. In our simple model we cannot hope to describe this effect adequately and incorporate it accurately. The most we can do is the following simple approximation.

In our we assume that the spatial distribution of radioactive nickel and cobalt is the same as for the mass density, (although we know that this is not the case for a real supernova). We have just found a prescription for calculating the quantity  $w=R_p/r_s$  as a function of  $y$ . Once we have  $w$ , we can calculate the fraction  $a(y)$  of the total mass that is inside the photosphere. Then according to our model  $a(y)$  should also be the fraction of the radioactive material inside the photosphere. Therefore a reasonable procedure might be to correct  $\delta$  as follows:

$$\delta \rightarrow \delta \cdot a[y(t)] \quad (4.70)$$

where

$$\begin{aligned}
a &= \frac{4\pi}{M_0} \int_0^{R_p} r^2 \rho dr \\
&= \frac{4\pi\rho_0 y^{-3} r_s^3}{\pi^{3/2} \rho_0 r_0^3} \int_0^w u^2 \exp(-u^2) du \\
&= \frac{4}{\pi^{1/2}} \int_0^w u^2 \exp(-u^2) du
\end{aligned} \tag{4.71}$$

Note from Fig. 16 that  $w \gg 1$  for early times when  $y$  is relatively small, but  $w$  decreases with time. Hence at early times  $a \approx 1$ , but it slowly decreases as time elapses.

#### 4.6 Model Supernova Light Curves

We're now ready to calculate light curves by means of the equation:

$$yy'' + \frac{1}{2}y'^2 + \left(1 - \frac{1}{y}\right) = \frac{1}{|\Omega_0|} \left[ E - \tau \int_0^{t/\tau} L dz' \right] \tag{4.72}$$

where:

$$\frac{E}{|\Omega_0|} = q \left[ 1 - \exp(-\lambda_1 t) + \delta \left( 1 - .26 \exp(-\lambda_2 t) - .74 \exp(-\lambda_3 t) \right) \right], \tag{4.73}$$

and where  $\delta$  is given by (4.35) and corrected by (4.70), (4.71),  $L$  is given by (4.52), and  $\tau$  is given by (4.15). We have the following free parameters at our disposal:  $q$  which is proportional to the strength of the explosion;  $f$  which is the fraction of solar mass in radioactive nickel,  $\kappa$  which is the opacity (assumed independent of temperature and density for simplicity), and  $t_1 = 1/\lambda_1$  which is the time constant for the explosion. We have calculated many solutions to (4.72) for various choices of the foregoing parameters. Rather than exhibiting them all, we will describe in words the general character of these solutions, and then exhibit two graphs for the most interesting case.

What do we want to know? For any given choice of parameters, we can find a solution of (4.72) as a function of  $z = t/\tau$  by numerical integration. From this solution we can determine the central density and temperature as a function of time, hence the density and temperature at any value of  $r$  and  $t$ . Thus we can determine the photospheric radius and temperature, hence the luminosity. The luminosity can be converted to an absolute magnitude, for example in V band, by applying a standard bolometric correction. We shall primarily be interested in plotting  $-M_V$  versus time, where  $M_V$  is the V band absolute magnitude, in addition to the photospheric temperature and radius.

What do we find?

- The quantities  $-M_V$ ,  $R_p$ , and  $T_{\text{eff}}$  are quite insensitive to  $t_1$  over a reasonably wide range (say between 10 and 10000 seconds). Thus for most calculations we have decided to assume the value  $t_1=100$  sec.
- We have varied the opacity  $\kappa$  over a wide range: from .02 to  $1.0 \text{ cm}^2\text{g}^{-1}$ . Now it is known from many observations of Type Ia Supernovae that at 25 days or so after peak luminosity, the effective temperature is approximately 5500 K. We find that our calculated effective temperature at 25 days after maximum is  $\approx 5500$  K if we choose  $\kappa=0.5$ . If  $\kappa \ll 0.5$ , the effective temperature at 25 days after peak is too high, while for  $\kappa > 0.5$  it is slightly too low.
- We know from our study of the zero-temperature white dwarfs that when  $M \approx M_C$  (the Chandrasekhar limit), the central density exceeds  $10^9 \text{ g/cm}^3$ , and a reasonable a priori choice is  $3 \cdot 10^9 \text{ g/cm}^3$ . In fact, we find that our computed results for  $-M_V$ ,  $R_p$ , and  $T_{\text{eff}}$  most nearly approximate actual Ia observations for the choice  $\rho_0 = 3.6 \cdot 10^9 \text{ g cm}^{-3}$ . This corresponds to  $\tau = 0.053$  s. and  $r_0 = 5.2 \cdot 10^7$  cm.
- We know from our preliminary studies of the differential equation (recall Sec. 4.3) that any real explosion must correspond to  $q > 1$ . We find best agreement between our computed values of  $-M_V$ ,  $R_p$ , and  $T_{\text{eff}}$  and real observations, when  $q \approx 1.5$ , although values of  $q$  between 1.35 and 1.7 are all more or less acceptable.
- The most interesting parameter is the nickel fraction  $f$ . In Fig. 18, we plot  $-M_V$  versus time in days for  $f = .2, .6$ , and  $1.2$  solar masses, assuming  $\kappa = 0.5$ ,  $q = 1.5$ , and  $\rho_0 = 3.6 \cdot 10^9 \text{ g cm}^{-3}$ , (called our “standard model” from now on.)

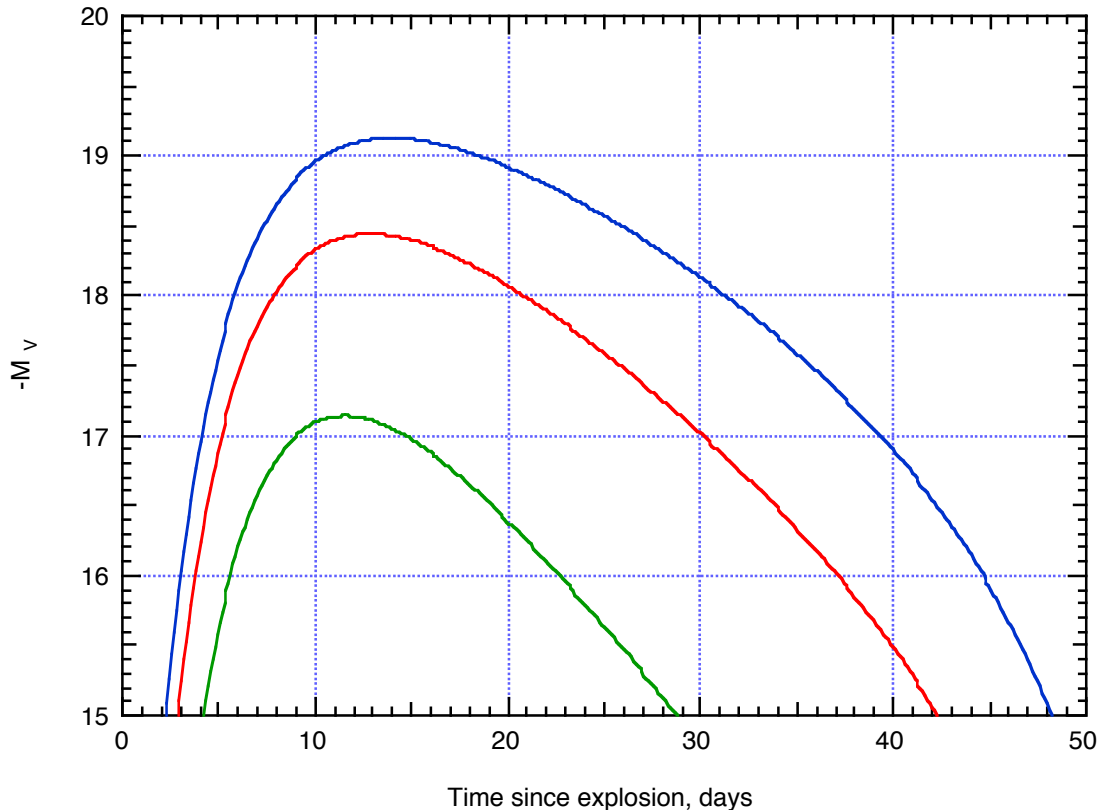


Fig. 18 Magnitude in V band versus time for  $f=0.2$  (green),  $0.6$  (red),  $1.2$  (blue). Given the extremely crude and simple nature of the model, the results shown in Fig. 18 are moderately encouraging. Each light curve peaks at about 10-20 days after explosion,

and the peak values are only  $\approx 0.5$  magnitude lower than in actual observations. The red curve drops by about 2.5 magnitudes in the first 25 days after explosion, in rough agreement with observations. There is even a suggestion of “stretch”, since the magnitude difference between successive curves increases with time. Of course we can’t expect too much from our calculation: in particular the model does not reproduce the nebular phase of real supernovae light curves; nor would this be expected since our treatment of opacity is so crude.

Fig. 19 shows the calculated photosphere radius as a function of time for  $f=0.6$ . We see here the same behavior already suggested in Fig. 17.

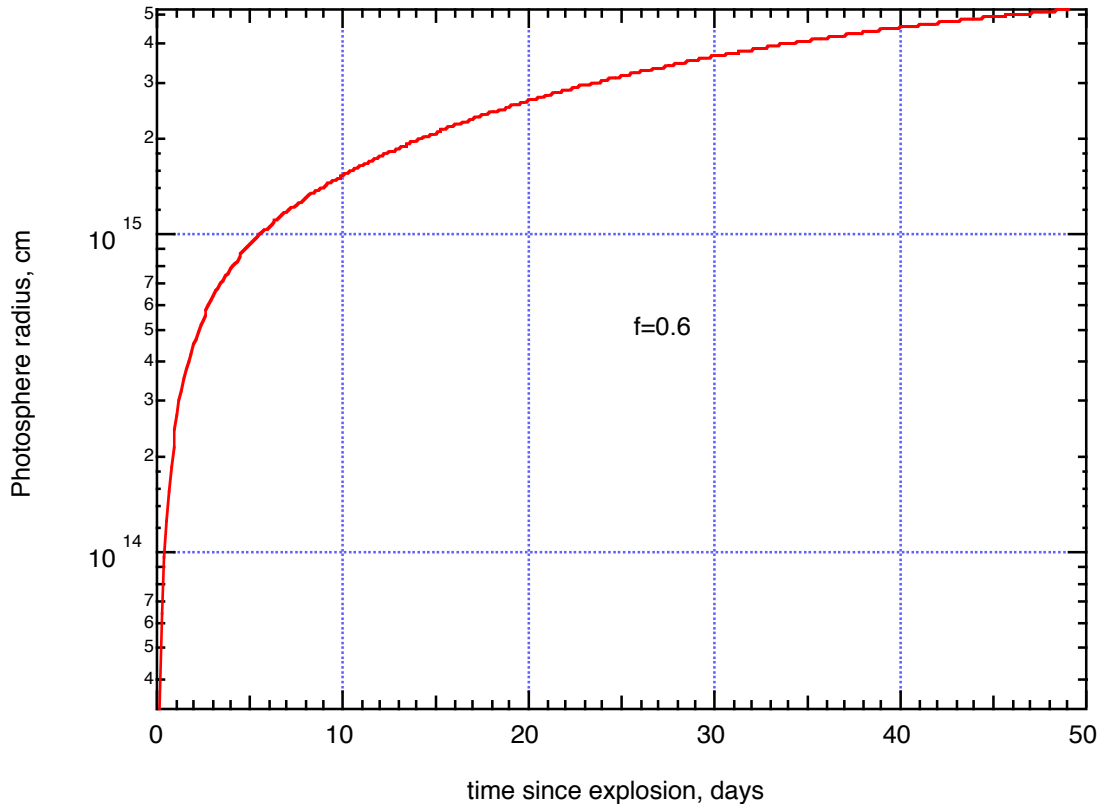


Fig. 19 Photosphere radius as a function of time for the standard model with  $f=0.6$ .

Mayer and Reitz have carried out calculations analogous to those just described, except that they ignored the luminosity loss term (second term on the RHS of (4.72)), ignored the “transparency effect” that corrects  $\delta$ , and arbitrarily fixed  $w=2$ , independent of  $y(t)$ . By doing so they obtained light curves that fit the observations somewhat better than do the results shown in Fig. 19. However, this better agreement must be considered completely fortuitous, since the luminosity loss effect is very important and cannot be ignored, while the other two effects are also significant.

To make further progress in our studies of Type Ia Supernovae using elementary methods, we shall turn in the next installment of these notes from the self-similar model to a more detailed look at the physics in the post-explosion supernova envelope. In particular we want to investigate how gamma ray energy from radioactive decay is converted to optical luminosity, and we want to study opacity in much more detail.





